

Anonymous Referee #1
Received and published: 19 August 2018

Overview:

Review of “XCO₂ in an emission hot-spot region: the COCCON Paris campaign 2015” by Vogel et al.

Vogel et al. present an analysis from a 2-week field campaign in Paris using the Collaborative Carbon Column Observing Network (COCCON). This network uses 5 FTIR spectrometers in and around Paris. The authors compare upwind and downwind concentrations from these spectrometers and use the CHIMERE-CAMS model to simulate XCO₂ at these sites. The campaign was hampered by poor meteorology and most of the results are from 4 days of measurements. Given this, the authors are unable to draw any major scientific conclusions but the work is nevertheless a nice demonstration of the viability of this kind of network. My main criticisms are that I feel this work is far too long (14 figures and 3 tables) given that another paper describes the construction of the network (Frey et al., AMTD) and the findings are rather limited given the meteorological limitations for this time period. Overall, I think the work should ultimately be published but could use major revisions to better justify the arguments that are novel. There are also a number of formatting and/or grammatical errors that should be addressed.

We have addressed the specific and general comments as well as addressed formatting issues. The text has been clarified and slightly re-focused and 4 figures and 2 tables were moved to the supplement. Original reviewer comments are given in blue with our response in black.

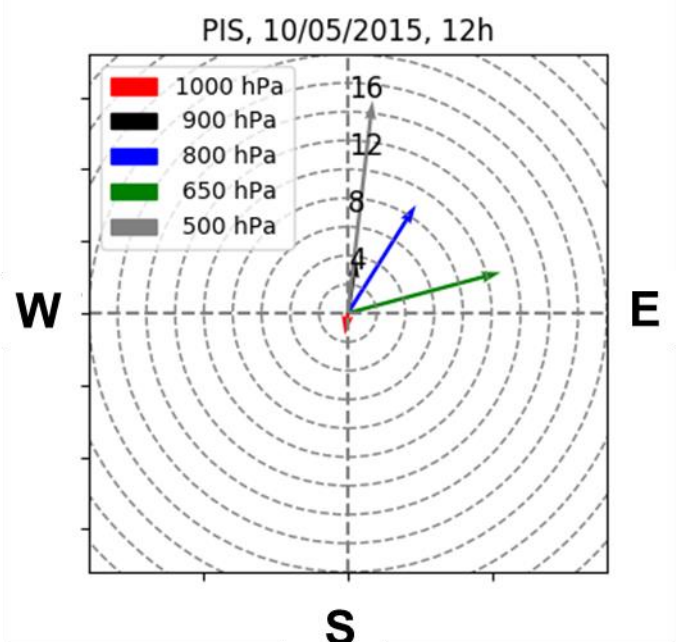
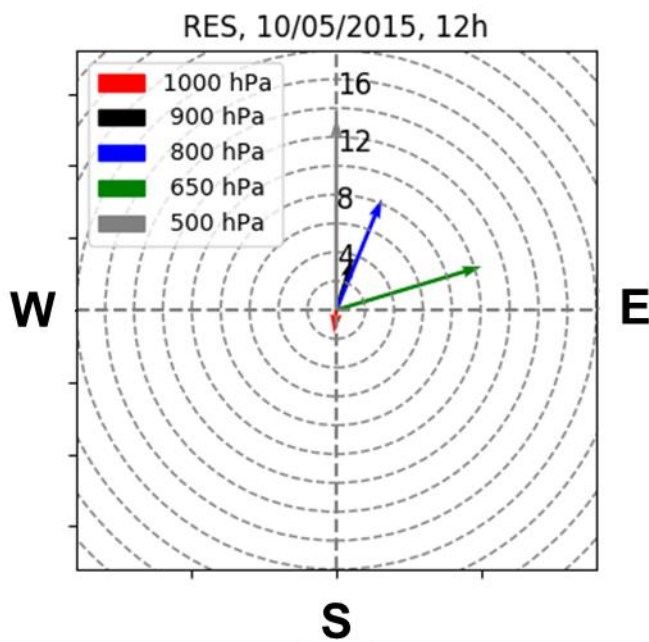
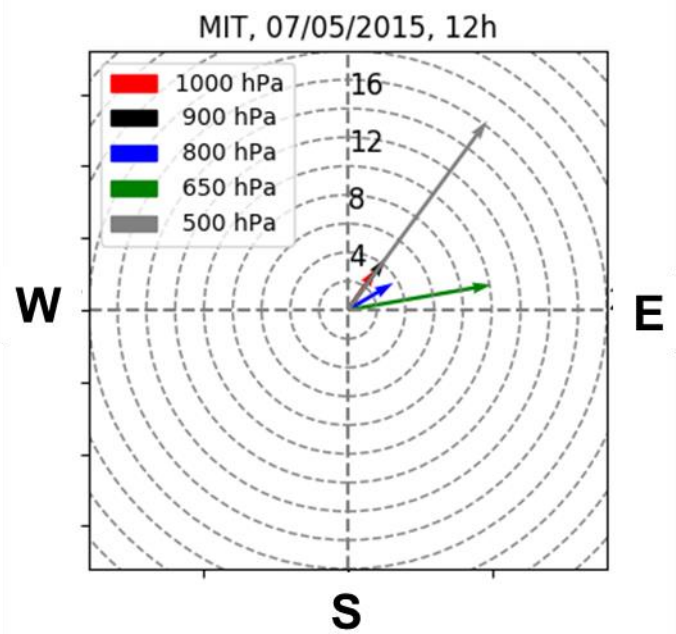
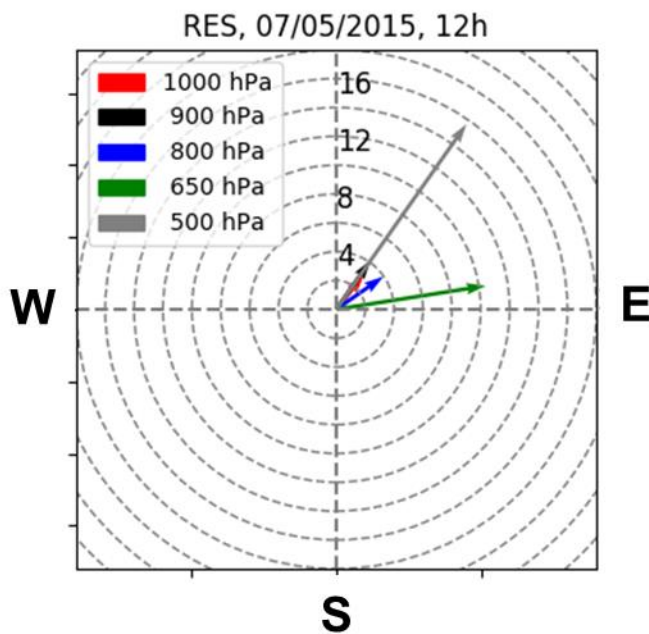
Comments:

I found myself struggling to characterize what I'm actually learning from the paper because the construction of the network is described in Frey et al. AMTD and previous work from this group has already shown the use of a gradient method in Breon et al. and Stauffer et al. To this reviewer, the major contribution is demonstrating that the gradient method can also work for column measurements and, to a lesser extent, that there is substantial uptake from the biosphere in an urban region like Paris. So I think the message of the paper could be better framed.

We did indeed highlight these aspects in the abstract, but we agree that it felt 'watered-down' in the main text of the initial manuscript. The manuscript has been streamlined and we have moved 4 figures and 2 tables into the supplement. Some more specific discussions and clarifications were added instead.

Additionally, the manuscript is actually rather weak in the demonstration that the gradient method is working for this region. For example, wouldn't wind shear also adversely impact the gradient method? If there is wind shear, you may have low-level winds that satisfy the upwind/downwind conditions but mid-to-upper tropospheric (or stratospheric?? Since it's a column measurement) winds that bring different background conditions. There is little discussion of this (or argument that it is not important in these cases). Are there radiosonde measurements or radar wind profiler data that could be used to demonstrate this?

Our model is based on ECWMF Integrated Forecast System (IFS) weather data, which has been demonstrated to compare fairly well with radiosonde data. We have added hodographs to show the wind-shear in the domain in the supplement (example also below).



As expected there are wind speed and direction changes in higher layers of the atmosphere. However, the wind conditions in higher layers (mid tropo-sphere and stratosphere) are not of key interest for this study as most of the XCO₂ variability is driven by the CO₂ mixing ratios in the boundary layer (typically well below 650hPa). The distance between upwind and downwind sites in our experiment is below 45km and there are no indications that significant concentration gradients exists in the stratosphere or even the mid/upper troposphere at this length-scale that would be comparable to the horizontal gradients within the PBL. Even in remote regions without strong urban CO₂ emissions vertical profiles are dominated by lower levels (below 650hPa) and

compare well with ECMWF-CAMS, which was used in this study as boundary condition (e.g. Membrive et al. 2017; <https://doi.org/10.5194/amt-10-2163-2017>)

We have added a discussion of wind-shear and why we have made the assumption that it is not a major influence (compared to other factors) here.

Overall, I think the manuscript would be far more useful if the authors were to move much of the discussion to a supplement and focus on the main findings. For example, many of the figures could be combined or reduced:

Thanks for this suggestion we have streamlined the manuscript.

- [Figs. 1 and 3 could be combined](#)

Thank you for the suggestion, we actually did try a combined graph before, but it was not easily readable. We have opted to move figure 3 into the supplement now.

- [It's unclear what Figure 4 is supposed to be telling me, Figure 5 seems to show the same data but in a much clearer form](#)

Figure 4 and 5 are indeed the same data, however, Figure 4 allows comparing how similar/different the XCO₂ variability is across different sites (spatial variability), while Figure 5 allows to assess the temporal XCO₂ variability at an individual sites.

- [Figures 8 and 9 could be combined into a 2-panel figure \(would facilitate a visual comparison\). However they could probably be moved to a supplement since I'm not sure if they're really necessary. It seems like Figure 10 does a better job of breaking down the contribution from various components \(which is actually rather interesting\)](#)

Agreed – we have moved Figure 8 into the supplement.

- [Table 3 could be in a supplement or cut since the locations are shown in Fig. 1.](#)

Specific comments:

Agreed – we have moved Table 3 into the supplement.

- [COCCON is in the title, isn't defined until page 3.](#)

We have added this information in the abstract.

[At the beginning of Section 3.1.2 \(Page 9\), the authors mention that the standard deviation for 1-minute data is 1 ppm. That seems huge given the changes that they're seeing. Does this mean the error bars on all their data points are \$\pm 1\$ ppm? I suspect there's something I am missing because that would make me rather skeptical of the results.](#)

This 1-ppm standard deviation is NOT the instrumental precision, but is driven by the variability of atmospheric conditions (in time and space). I.e. all minute data were used to calculate the mean concentration of the campaign period and their variability is 1ppm. We have added text to clarify the issue.

- [Page 2, Lines 64–67: Just because one single factor doesn't explain the variations between cities doesn't necessarily mean it's uncertain.](#)

This criticism is not completely clear. We did not claim (and don't want to) that the uncertainty of emissions is caused by the fact that urban emissions cannot be explainable by a simple factor, but we rather wanted to highlight that cities cannot be generalized and need to be investigated individually. We have added wording to make it more clear and avoid confusion.

Page 2, Lines 70–73: Should give references to these other networks.

These networks were referenced in line 74. We have moved the references to clarify and we also added other relevant references.

Page 2, Line 74: Urban measurements are representative of a 10000 km² region?? I'm rather skeptical of that.

The Ile-de-France region (surrounding Grand Paris) is 12'012km² and the atmospheric GHG and air pollutant composition in this region is often dominated by Parisian emissions, which are constraint by regional observations (Breon et al. 2015 and Staufer et al. 2016). Furthermore, our measurements are conducted in the outskirts of the urban area to not be influenced by local sources only, but to be sensitive to the larger area. We have added text to clarify.

Page 3, Lines 93–95: The recently funded GeoCARB satellite is a geostationary satellite that will have multiple measurements per day.

Thanks, we have clarified this here.

Page 3, Lines 108–110: Again, this applies to LEO satellites but there are upcoming GEO satellites as well.

We specifically mentioned LEOs in line 107 and GEOs in line 112. Where we highlighted that GEOs are not restricted to the LEO time window.

Page 4, Lines 113: Should add the O'Brien et al. AMT (2016) paper because this satellite is actually funded.

We have added the reference to GEOCARB here. (O'Brien was also cited in line 89 of the original manuscript).

Page 4, Line 137: Would be good to flip the order of "airports" and "industrial" because it looks like AIRPARIF just refers to airports (since it starts with AIR).

We have added an explanation here. AIRPARIF is the air quality association that monitors/manages the airshed of Paris. It is not related to the airports agency of Paris (PARIS AEROPORT).

Page 6, Lines 191–195: Impressive!

Removed "impressive" and we will leave it to the readers to judge the performance – sometimes good results get the (co-)authors excited.

Page 7, Line 231: Missing subscript, should be "CO₂". Authors should do a search and replace because there are many instances of incorrect subscripting for CO₂.

We have corrected all CO₂ and XCO₂ and FFCO₂ to have correct subscripts.

Page 8, Lines 276–293: This nomenclature is very confusing. There are subscripts and superscripts on many variables and some of the variables have multiple letters (e.g., "COs₂_model" is not a great variable name). Would be much better if the authors used standard nomenclature from either Rodgers (2000) or the TCCON group. Either would be preferable to the current.

Although we agree that multiple having sub-scripts and super-scripts in equation are suboptimal when considering readability, this is also the case in TCCON publications, e.g. Kuai et al. 2013 (doi:10.5194/amt-6-63-2013). The nomenclature, here, was chosen to be consistent with previous COCCON publications, but we would definitely encourage that a common nomenclature is established across different remote sensing efforts/networks.

Page 8, Line 283: Why is WACCM bolded? Is it supposed to be a matrix (those are the only other bolded terms).

Corrected

Page 9, Lines 316–317: How are these spectra rated? Unclear

The quality of the data for each day was rated according to the overall data availability and similar to the previously published work by Hase et al. 2015 www.atmos-meas-tech.net/8/3059/2015/. We have added the reference.

Page 9, Lines 328–329: Upwind is higher concentration?? Probably a typo, I think you meant downwind. . .

Yes, thanks for catching this -> corrected

Page 10, Lines 337–338: Are there no other factors?? That seems surprising. Would wind shear or variations in winds, a decreasing anthropogenic source during the day not be able to give decrease? Needs stronger justification w/ data or citations.

We have corrected this sentence as other factors could contribute. However, our simulation attribute the decrease of CO₂ to NEE (uptake) within the domain, but the underlying biospheric fluxes could indeed be wrong.

Page 10, Lines 341–344: This doesn't seem supported by the analysis. I'd like to see a footprint analysis or some other way for this to be justified. . .

Our modelling framework does not provide footprints and running a lagrangian model in addition to CHIMERE is beyond the scope of this work. We have added citations of other studies where XCO₂ column footprints were investigated.

Section 3.13 Page 10: What about wind shear? Were there any radiosondes that indicate the winds are uniform through the column? What about the model? Does that indicate uniform winds throughout the column.

See general comment on wind shear and hodographs

Page 10, Lines 361–365: How representative are the winds at GIF? This could easily be tested in the model, (e.g., look at how variable the winds are over Paris and compare that to the grid cell w/ GIF).

Looking at the hodographs for the lower model levels they seem very consistent across Paris

Page 11, Lines 395–397: Couldn't you just coarsen the 1km inventory and then do this comparison?

Sorry, this point was not very clear. We cannot compare different anthropogenic emission products in this study as no other 'inventories' are available at this resolution. Coarsening IER to the resolution of e.g. EDGAR V4.2 would not still not yield a fair comparison to assess the performance/influence of the spatial disaggregation at the 2x2km² scale. We have added text to clarify this point.

Page 12, Lines 413–415: How are you directly linking this to NEE? Seems like this needs more justification.

We have added clarification. In our model FFCO₂, NEE and BC are transported separately, so we can directly see which source has contributed CO₂ to our simulated XCO₂ in our domain.

Page 13, Lines 475–476: How is this being assessed? Does the model agree with this (i.e. is the modeled contribution the same at each site)?

Yes, the model predicts similar biogenic contributions and we ASSUME that the influence of rural biogenic fluxes in our domain affect our sites in a similar way. We have added text to clarify.

Page 14, Line 492: Would prefer the authors not use “BC” here, was confusing at first read because of NEE abbreviation right before.

Change to ... and boundary conditions (i.e. the influence of CO₂ being transported into our domain) only....

Page 14, Lines 501–503: Couldn't the model transport also be wrong?

This is a definite yes – the transport model could be wrong. Our reasoning not to assume that this is the dominant factor here is that a.) the wind observations are well reproduced by CHIMERE, see figure 7 and b.) the PIS-RES gradient falls onto the 1:1 line - compared to the 1.7 of MIT-RES. It seems unlikely that the model properly models transport from RES to PIS but fails for RES to MIT as there a no major topographic disturbance in this part of the Paris Basin. We have added a note of caution that the model could be wrong in the discussion, as well as why we think this is not the biggest contributor to the disagreement here.

Anonymous Referee #3

Received and published: 6 November 2018

General Comments

This manuscript describes a pilot project of five EM27/SUN spectrometers that were deployed for two weeks in the Paris region to investigate CO₂ fluxes from that megacity. They also describe a modeling framework to compare to the column measurements and provide some initial comparisons. While it is commendable that the authors are publishing the results of a pilot phase of a project where important details about the instrumentation are shown, their analysis is incomplete. The “background” on the modeled result was very different from the observations, and no hypothesis was given for why that might be the case. Then, the analysis and discussion behind Fig 13 and 14 had several logical gaps and should be completely reconsidered. The conclusions section had several problems and was not well supported by the main text.

I do not think it would take that much work to fix these issues, but they are major issues with the analysis and interpretation of the study. Until these are fixed I would not recommend publication. We have significantly streamlined the paper and also expanded on our analysis of the data to fill the gaps identified by the reviewer.

Specifically, we have added more explanation/interpretation around Figures 13 and 14 and clarified the text to avoid misunderstandings (e.g. Figure 14 is already the mean daily cycle for selected data i.e. when the site is an upwind site). More explanation in individual improvements and corrections is given below.

Specific Comments

Line 92: remove the word “by”.

Corrected – Thanks.

Line 105: “spectrometers” should be singular, ie “spectrometer”

Corrected - Thanks

Line 111: This sentence is grammatically incorrect and should be reworded slightly.

We have reformulated this sentence.

Line 153: remove the word “for”

Corrected - Thanks

Line 154: Add “PM” at the end of the line.

Corrected - Thanks

Line 192: Does instrument 1 have the best agreement with the TCCON instrument? The text here and in the rest of the paragraph indicates that the EM27/SUN measurements CAN be made traceable to the WMO scale, but it doesn't say IF they were or not. It would be good to explain if they were, and if they were not it is even more important to say that and explain why they were not.

There is nothing special about spectrometer #1, arbitrarily one of the devices has been used as reference here. Any drift of the calibration in either the selected reference spectrometer or of one of the other spectrometers would induce variations in the table entries (correlated between different spectrometers if the reference is drifting, uncorrelated if one of the other spectrometer is drifting)

The measurements can be made traceable to WMO scale to the extent that can be achieved for TCCON. Direct side-by-side comparison with a TCCON spectrometer have been used to estimate the calibration offset of the EM27/SUN wrt TCCON. As the same spectral bands are used for the observations and the instrumental characteristics of both TCCON and EM27/SUN spectrometers are very close to an ideal FTS, it is expected that the calibration between EM27/SUN and TCCON is quite consistent. The paper of Frey et al. provides a good impression of the level of consistency found. (Frey, M., Sha, M. K., Hase, F., Kiel, M., Blumenstock, T., Harig, R., Surawicz, G., Deutscher, N. M., Shiomi, K., Franklin, J., Bösch, H., Chen, J., Grutter, M., Ohyama, H., Sun, Y., Butz, A., Mengistu Tsidu, G., Ene, D., Wunch, D., Cao, Z., Garcia, O., Ramonet, M., Vogel, F., and Orphal, J.: Building the COllaborative Carbon Column Observing Network (COCCON): Long term stability and ensemble performance of the EM27/SUN Fourier transform spectrometer, Atmos. Meas. Tech. Discuss., <https://doi.org/10.5194/amt-2018-146>) However, we would not want to claim that this data is traceable to WMO, yet as more comparison and methodological work should be done in the future.

Line 328-331: I think the authors got this backwards, the text says that the upwind sites had higher XCO₂ than their downwind sites indicating that the FFCO₂ from Paris is detectable. I think they meant to switch upwind and downwind.

Yes, indeed we somehow switched this and failed to notice in proof-reading. Thanks for catching this.

Another comment about these lines is that, looking at Fig 4, it looks like RES is lower than MIT for most of the study period, but this switches on May 12/13 and RES is higher than MIT. This makes perfect sense looking at Table 3 where it says that for the first part of the campaign the winds were predominantly from the SW while on the 12/13 the winds were from the NNW and NE. It might be worth explaining this feature in the data here since its interesting.

We have added more discussion on this.

Line 350: The word “northeasterly” is used incorrectly here. Change this to “The two (typically downwind) sites PIS and MIT northeast of Paris show a . . . ”

Corrected

Line 351: What does the word “background” mean in this context? Background could mean several things in this context, so I would encourage the authors to either define what the background is or use a different word here to avoid confusion.

We have removed the word background here as it is indeed confusing and means different things in different communities. We have given more specific explanations when necessary.

Line 356: The word “background” is used again with, I think, a different meaning than was used above. It is also undefined here. I understand exactly what the authors mean, but I think it would be good to provide a little bit of explanation here describing exactly what they mean by background conditions (ie the XCO₂ of the air mass entering the urban domain that has been affected by emissions upwind or outside of the domain).

We have removed the word background here as it means different things in different communities – even among the co-authors of this paper. We have added an explanation of the assumption underlying the gradient approach.

Line 360: “are” should be “were”.

Corrected

Line 361: “measurement period” should be “on this day” since the winds do vary over

the whole measurement period, but they were from the SW on this day that is the focus of this figure.

Corrected

Line 362: This sentence needs to be re-written for clarity. How about this: "The observations from GIF showed only minimal differences with RES while the rest of the sites (PIS, JUS, and MIT) had Δ values of 1 to 1.5 ppm.

Thanks for this suggested - corrected

Line 363: Delete "of most"

Corrected

Lines 355-376: Be careful of the tense in this paragraph and elsewhere. For most of the paper the data was referred to in the past tense, but I noticed that this paragraph is in the present tense. To fix this, change "is" to "was" (etc) when referring to the data throughout the section. Thanks – this error was corrected (all in past tense, where appropriate).

Lines 405: On this line I initially thought that the authors were drawing a comparison between the modeled XCO₂ and the measured XCO₂, but after reading the sentence several times I now realize they are just talking about modeled XCO₂. It would be good to explicitly say "modeled XCO₂" on line 405 to prevent any confusion.

The paragraphs were explicitly separated into measured and modelled to avoid confusion, but we've now added more clarifying markers in the paragraph.

Lines 413-415: Might also be worth pointing out that sometimes the NEE flux is slightly positive due to respiration, generally at night.

We've added an explanation.

Line 424: I don't see any shaded areas on Fig 11.

Removed the mention of the grey shaded area as the wind directions are given on top of graph 11.

Lines 420-436 (and Fig 11): After reading this a couple of times and staring at Fig 11, I finally realized that each of the vertical panels represents a different modeled source. The subscripts on the y-axis are very small and are not explained anywhere. It would be good to explain what each of the panels are showing in the figure caption. The authors should also explain in the text that this figure shows the total XCO₂ in the top panel, and below that the three panels show the modeled contributions from FFCO₂, biological emissions (NEE), and background conditions (BC) respectively.

We have increased the size of the labels and added more explanation in the caption to make the information more accessible to the reader.

Line 440: They should reference Fig 12 at the beginning of this paragraph somewhere.

Figure 12 were references in line 444 now moved to line 440.

Line 441: There is an extra period and spaces on this line.

Removed

Line 445: I would encourage the authors to not the background offset FIRST in this paragraph as that is the most obvious feature. Then, once the offset is noted they can go on to describe the diel cycle and the difference between the sites.

Also, the authors should offer an explanation for why they think their background model is 1-2 ppm off.

We have restructured this paragraph and also added the information about the reduced impact of BC when using the gradient approach.

Line 454: The authors should explain here that this comparison is not sensitive to the offset in the BC because it is comparing the modeled upwind with the modeled downwind and the measured upwind with the measured downwind.

Also, as a general note, the use of the delta symbol is problematic because of its use in radiocarbon nomenclature. It's OK if the authors desire to use it, but I would encourage them to find an alternative way of noting this.

See reply to comment on line 445.

Concerning, the general note on nomenclature, as radiocarbon is not mentioned in this manuscript and the remote sensing community does not commonly use $\Delta^{14}\text{C}$ we decided to use this nomenclature as it seemed most appropriate to the (co-) authors.

Line 452-465: I really don't understand what the significance of Fig 13 is, and this analysis doesn't make sense to me. I would expect that the observations should only fall on the 1-1 line when the wind direction is directly between the upwind/downwind sites. The fact that most of the observations have a slope close to 1 could alternatively suggest that wind direction doesn't matter! I would also expect that when the wind direction is from a 90-degree angle to the upwind direction (so that the wind is blowing across the city instead of from one site to the other) that there should be much higher variability and potentially no relationship between the XCO₂ at the two sites.

We have added additional elements to better explain figure 13. Fundamentally, the point was to investigate the impact of wind direction on the concentration gradient and if our atmospheric transport model predicts concentrations equally well for all wind conditions. Apparently these messages were lost/unclear. As expected the gradients are strongly positive when MIT and PIS are downwind of Paris and we see negative gradients when they are upwind. Furthermore, the slope of the individual wind-directions does not seem to follow the 1:1 line. Especially, northerly winds (blue colors in Fig13 – now Fig 9) seem to have steeper slopes for PIS. This figure also highlights that when trying to assess the impact of Parisian emissions significant gains in signal amplitude can be gained when using data from upwind-downwind situations only. This is not really a 'surprising' finding, but we can now quantify how much more signal is seen on average. On the 90 degree question – even in this situation with easterly winds we could expect to see differences. As shown in Figure 1, the RES site is then and MIT is technically upwind, which explains the negative gradient in Figure 13. The gradient for west however is quite different then for Northerly winds as other parts of Paris are then "upwind" of RES

As the reviewers will find, we have added much more explanation and interpretation around Figure 13 to clarify our interpretation.

Here are a few suggestions for Fig 13. The authors should only plot the data from when the wind is blowing directly from PIS->RES (or MIT->RES) and when it is blowing back from PIS<-RES (or MIT<-RES). There should only be a narrow range of wind direction angles that this comparison should work, maybe 20-30 degrees or something like that. Also, the authors should indicate on the figure, or in the text somewhere what the exact angle it is between the sites in decimal degrees (not just with letters indicating the cardinal directions). Also, the figure caption says that the vertical bars indicate the standard deviation, but they don't say WHAT it's the standard deviation of! Is it the standard deviation of the measurements from a range of wind directions? Is it over some time window?

Thanks for the suggestions. We have added exact bearings and distances of all stations relative to RES in table S1 in the supplement. We have kept Figure 13 as it allows seeing the influence of different wind conditions on the concentration gradients. A narrow upwind/downwind window would not allow seeing this and would also remove a lot of the data. We think the color-code in figure 13 allows to see how certain wind conditions are pooled. PIS is optimally upwind of RES at a wind direction of 187 degrees (green) and MIT is optimally upwind for a wind direction of 217 degree (green).

Lines 466-479: This diurnal cycle plot is confusing to me because there are times when the wind is blowing from PIS to RES, and there are times when the wind is blowing in the opposite direction. Shouldn't the XCO₂ be negative when it is blowing in the opposite direction? Wouldn't it also have no relationship between the sites when there is no upwind/downwind relationship? It would be much better to isolate this comparison to ONLY times when the wind is blowing in the appropriate direction, not during the whole campaign.

This plot DOES indeed only include data when MIT and PIS are downwind of RES. For the observations (upper panel) only data from days with observations are used. This is also why only so few days (0 to 5) contribute to the mean diurnal cycle (as given by the labels on top panel of Figure 14) In the lower panel all days within the campaign period that fulfill the upwind-downwind requirement are used. We have added text to clarify this.

Line 482: "two-weeks" should be "two-week".
Corrected

Line 485: What do the authors mean by "easily linked"? This is sloppy language that is easily misinterpreted, especially in the conclusions section. This whole sentence needs to be re-written for clarity so that the wrong impression is not given.
We have reformulated to clarify.

Line 488: The authors don't actually know what is impacting remote CO₂. This should instead say something like ". . . greatly reduced the impact of background CO₂ fluxes."
Thanks – we have reformulated to clarify. Using the gradient does indeed reduce both the influence of boundary condition CO₂ and biogenic fluxes within the CHIMERE domain

Line 491: the word "significant" has statistical meaning and shouldn't be used in this instance. Also, "enhanced background" seems incorrect since they never offered a hypothesis about why the background was higher. Actually, just the word "enhanced" should be changed to "higher" or something that is more objective.
We have reformulated and change the wording where appropriate.

Line 492: Here is the word "significantly" again. The authors should use a different word here, like ". . . also predicts that NEE and BC only has a large impact on XCO₂ during a few situations . . ."
We have reformulated and change the wording where appropriate.

Lines 491-494: Actually, this whole sentence is problematic and needs revision. The first half of the sentence seems to refer to the discussion surrounding Fig 10 (which is great) but the second half of the sentence referring to upwind and downwind (as it relates to NEE and BC) seems unrelated. If this stays in the text, it needs more detail to explain what the authors were thinking about.
We have reformulated to clarify.

Line 494-496: This section refers to Fig 13, and this methodology is flawed since an alternative explanation is that wind direction doesn't even matter in this data set.

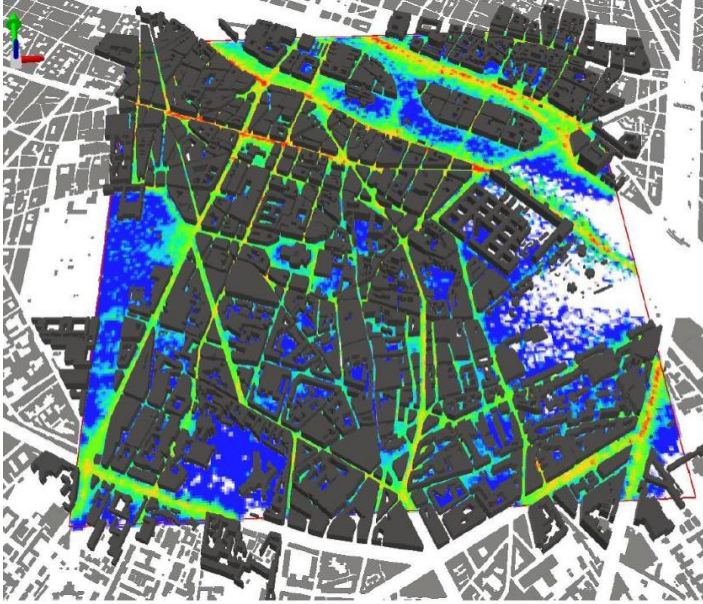
Unfortunately, we can't really follow why the wind directions do not matter in this data set. It seems apparent that southerly winds produce strong positive concentration offsets, while northerly winds cause negative concentration gradients. Looking at the colors they seem to group very consistently implying a strong correlation of wind conditions on ΔXCO_2 , both modelled and observed. The slope is not wind dependent, but it is not clear why it should be, as we assume that the model performance should be similar in all wind conditions

Line 496-498: This is wrong. I assume they are referring to Breon et al 2015 Fig 6 where the highest $R = 0.90$ (not 0.91). Also, this was a straight measured/modeled mole fraction comparison, whereas the analysis in Fig 13 is supposedly the up-wind/downwind measured/modeled gradient. Even if the analysis in Fig 13 were done correctly, this would be a different metric for model evaluation and should not be compared with Breon et al 2015. Its comparing apples (measured/modeled in-situ mole fractions) and oranges (measured/modeled GRADIENTS BETWEEN SITES across a city during a 2-week period with a lot of wind direction changes).

Concerning Breon et al. 2015: that study also compared measured and modelled in-situ CO_2 gradients between sites across the city for a period of 4 weeks see figures 8, S4 and section 4.4. (<https://www.atmos-chem-phys.net/15/1707/2015/acp-15-1707-2015.pdf>). R_2 for GIF and GON gradients is 0.91 as previously mentioned in the manuscript. The sites chosen in our COCCON campaign are also similar to the locations used in Breon et al. 2015. Some of the (co-)author of this study are indeed (co-)authors of Breon et al. 2015 and although it might not be exactly an 'apples to apples' comparison when comparing in-situ CO_2 gradients to XCO_2 gradients we wanted to cite this study to show that we are attempting to applying an analogous approach.

Line 498-505: This whole section needs to be redone after the analysis in Fig 13 is fixed. Also, the speculation about model dispersion is not based on anything and therefore it has no place in the paper unless the authors care to actually try to do some analysis to quantify it.

We have re-worked this section. The hypothesis that the dispersion is an issue is indeed only based on experience using the CHIMERE model and the fact that the model resolution is limited to $2 \times 2 km^2$ which leads to numerical diffusion that is very likely larger than real dispersion. In a recent study, model simulations of CO_2 in the boundary layer of Paris at $5m \times 5m$ resolution were performed using MICRO-SWIFT-SPRAY. A lot of heterogeneity is visible (the Figure below is a $2 \times 2 km^2$ pixel of downtown Paris: Jardin du Luxembourg to Jussieu with the Seine River in the top of domain).



Such localized sources and plumes are immediately dispersed within a 2x2km² CHIMERE cell.

Line 509-511: I actually agree with this statement, but it's exactly the opposite of what the analysis in this paper shows. Fig 11 shows that the biospheric flux in a gradient sense is small (less than 1ppm almost all the time).

We have clarified that the influence of the biosphere on XCO₂ is a major factor but not as important when considering Δ XCO₂ here. The point we want to make is that biospheric fluxes are not always important, however there are periods when they cannot be ignored, even when using a gradient approach.

Line 514: They forgot the word "not". It should be "... and underlying fluxes could NOT be investigated here."

Corrected

Line 522: I would disagree that they have demonstrated that the modeling framework is "suitable". They have provided some initial modeling results from a pilot test field campaign and the modeling framework will need a lot of work before it can be usefully applied to interpret fluxes.

We have reformulated to highlight that we also see this as a step forward towards our inversion system.

Figure 3: The x and y axes should be labeled longitude and latitude.

We've moved the figure into the supplement and made it bigger (also the lat-long labels)

Figure 7 (top): the y-axis scale could be 0-10 instead of 0-16.

Figure 8: The acronym MACC is not defined anywhere in the manuscript.

Thanks – we've added this information in the caption

Figure 10: In the caption the authors should add "(BC)" so that the reader knows that the legend entry "CHIMERE BC only" means background conditions.

Corrected

1 **XCO₂ in an emission hot-spot region: the COCCON Paris campaign 2015**

2

3 F.R. Vogel^{1,a}, M. Frey², J. Stauffer^{3,a}, F. Hase², G. Broquet⁴, I. Xueref-Remy^{5,a}, F. Chevallier⁴,
4 P. Ciais⁴, M. K. Sha^{6,b}, P. Chelin⁷, P. Jeseck⁸, C. Janssen, Y. V. Te⁸, J. Groß², T.
5 Blumenstock², Q. Tu² and J. Orpha²

6

7 1. Climate Research Division, Environment and Climate Change Canada, Toronto, Canada

8 2. Karlsruhe Institute of Technology (KIT), Institute of Meteorology and Climate Research
9 (IMK), Karlsruhe, Germany

10 3. Thales Services, Regional Competence Center Aerospace and Science Engineering,
11 Toulouse, France

12 4. Laboratoire des Sciences du Climat et de l'Environnement (LSCE), IPSL, CEA-CNRS-
13 UVSQ, Université Paris-Saclay, Gif-Sur-Yvette, France

14 5. Observatoire de Haute Provence, OSU Pytheas, Saint-Michel l'Observatoire, France

15 6. Royal Belgian Institute for Space Aeronomy, Brussels, Belgium

16 7. Laboratoire Inter-Universitaire des Systèmes Atmosphériques (LISA), (CNRS UMR 7583,
17 Université Paris Est Créteil, Université Paris Diderot, Institut Pierre Simon Laplace), Créteil,
18 France.

19 8. Laboratoire d'Études du Rayonnement et de la Matière en Astrophysique et Atmosphères
20 (LERMA), IPSL, Sorbonne Universités, (CNRS, PSL Research University, Observatoire de
21 Paris), Paris, France

22

23 Previously at

24 a. Laboratoire des Sciences du Climat et de l'Environnement (LSCE), IPSL, CEA-CNRS-
25 UVSQ, Université Paris-Saclay, Gif-Sur-Yvette, France

26 b. Karlsruhe Institute of Technology (KIT), Institute of Meteorology and Climate Research
27 (IMK), Karlsruhe, Germany

28

29 *Correspondence to: Felix R. Vogel (Felix.Vogel@canada.ca)*

30

31 **Abstract.** Providing timely information on urban Greenhouse-Gas (GHG) emissions and their
32 trends to stakeholders relies on reliable measurements of atmospheric concentrations and the
33 understanding of how local emissions and atmospheric transport influence these
34 observations.

35 Portable Fourier Transform Infra-Red (FTIR) spectrometers were deployed at 5 stations in the
36 Paris metropolitan area to provide column-averaged concentrations of CO₂ (XCO₂) during a
37 field campaign in spring of 2015, as part of the Collaborative Carbon Column Observing

38 [Network \(COCCON\)](#). Here, we describe and analyze the variations of XCO₂ observed at
39 different sites and how they changed over time. We find that observations upwind and
40 downwind of the city centre differ significantly in their XCO₂ concentrations, while the overall
41 variability of the daily cycle is similar, i.e., increasing during night-time with a strong decrease
42 (typically 2-3 ppm) during the afternoon.

43 An atmospheric transport model framework (CHIMERE-CAMS) was used to simulate XCO₂
44 and predict the same behaviour seen in the observations, which supports key findings, e.g.
45 that even in a densely populated region like Paris (over 12 Million people), biospheric uptake
46 of CO₂ can be of major influence on daily XCO₂ variations. Despite a general offset between
47 modelled and observed XCO₂, the model correctly predicts the impact of the meteorological
48 parameters (e.g. wind direction and speed) on the concentration gradients between different
49 stations. Looking at the local gradients of XCO₂ for upwind and downwind station pairs, ~~which~~
50 ~~is found to be~~ less sensitive to changes in XCO₂ ~~regional background-boundary~~ conditions
51 ~~and biogenic fluxes within the domain and~~, we find the model-data agreement ~~significantly~~
52 ~~further improves~~~~better~~. Our modelling framework indicates that the local XCO₂ gradient
53 between the stations is dominated by the fossil fuel CO₂ signal of the Paris metropolitan area.
54 This ~~further~~ highlights the ~~potential~~ usefulness of XCO₂ observations to help optimise future
55 urban GHG emission estimates.

57 1 Introduction

58 Atmospheric background concentrations of CO₂ measured since 1958 in Mauna Loa, USA,
59 have passed the symbolic milestone of 400 ppm (monthly mean) as of 2013 [Jones 2013].
60 Properly quantifying fossil fuel CO₂ emissions (FFCO₂) can contribute to define effective
61 climate mitigation strategies. Focussing our attention on cities is a critical part of this
62 endeavour as emissions from urban areas are currently estimated to represent from 53 % to
63 87 % of global FFCO₂, depending on the accounting method considered, and are predicted to
64 increase further [IPCC-WG3 2014, IEA 2008, Dhakal 2009]. As stated in the IPCC 5th
65 assessment report, "*current and future urbanisations trends are significantly different from the*
66 *past*" and "*no single factor explains variations in per-capita emissions across cities and there*
67 *are significant differences in per capita greenhouse gas (GHG) emissions between cities*
68 *within a single country*" [IPCC-WG3 2014]. ~~Therefore, findings in one city cannot often not be~~
69 ~~simply used and extrapolated to other urban regions. Furthermore, T~~the large uncertainty of
70 the global contribution of urban areas to CO₂ emissions today and in the future is why a new
71 generation of city-scale observing and modelling systems are needed.

72 In recent years, more and more atmospheric networks have emerged that observe GHG
73 concentrations using the atmosphere as a large-scale integrator, for example in Paris,
74 ~~(France)~~ ~~(e.g., Bréon et al. 2015, Xueref-Remy et al, 2018)~~, Indianapolis, ~~(USA)~~ ~~(e.g. Turnbull~~

75 [et al. 2015, Lauvaux et al. 2016](#)), Salt Lake City, USA ([Strong et al. 2011, Mitchell et al. 2018](#)),
76 [Heidelberg, Germany](#) (e.g. [Levin et al. 2011, Vogel et al. 2013](#)) and Toronto, ~~(Canada)~~
77 [\(e.g. Vogel et al. 2012\)](#). The air measured at in-situ ground-based stations is considered to be
78 representative of surface CO₂ fluxes of a larger surrounding area (1 km²-10000 km²) [, i.e. the](#)
79 [emissions of the Greater Paris Area dominate the airshed of the Ile-de-France \(ca. 12'000](#)
80 [km²\)](#)~~(e.g., Bréon et al. 2015, Xueref-Remy et al., 2018), Turnbull et al. 2015, Vogel et al. 2013]~~
81 [\(Staufer et al. 2016\)](#). If CO₂ measurements are performed both up-wind and downwind of a
82 city, the concentration gradient between the two locations is influenced by the local net
83 emission strength between both sites and atmospheric mixing [[Xueref-Remy et al, 2018,](#)
84 [Bréon et al. 2015, Turnbull et al. 2015](#)]. To derive quantitative flux estimates, measured
85 concentration data are typically assimilated into numerical atmospheric transport models
86 which calculate the impact of atmospheric mixing on concentration gradients for a given flux
87 space-time distribution. Such a data assimilation framework implemented for Paris with three
88 atmospheric CO₂ measurement sites [[Xueref-Remy et al, 2018](#)] previously allowed deriving
89 quantitative estimates of monthly emissions and their uncertainties over one year [[Staufer et](#)
90 [al. 2016](#)].

91 Space-borne measurements of the column-average dry air mole fraction of CO₂ (XCO₂) are
92 increasingly considered for the monitoring of urban CO₂. This potential was shown with OCO-
93 2 and GOSAT XCO₂ measurements, even though the spatial coverage and temporal sampling
94 frequency of these two instruments were not optimized for FFCO₂ [[Kort et al., 2012,](#)
95 [Janardanan et al. 2016, Schwandner et al. 2017](#)], while other space-borne sensors dedicated
96 to FFCO₂ and with an imaging capability are in preparation [[O'Brien et al, 2016, Broquet et al.](#)
97 [2017](#)]. Important challenges of satellite measurements are that they are not as accurate as in-
98 situ ones, having larger ~~by~~ systematic errors, while the XCO₂ gradients in the column are
99 typically 7-8 times smaller than in the boundary layer. Another difficulty of space-borne
100 imagery with passive instruments is that they will only sample city XCO₂ plumes during clear
101 sky conditions [for geostationary satellites and with an additional constraint to observations](#) at
102 around mid-day [for low-earth orbiting satellites](#).

103 The recent development of a robust portable ground-based FTIR (Fourier Transform InfraRed)
104 spectrometer as described in [Gisi et al. \[2012\]](#) and [Hase et al. \[2015\]](#) (EM27/SUN, Bruker
105 Optik, Germany) greatly facilitates the measurement of XCO₂ from the surface, with better
106 accuracy than from space and with the possibility of continuous daytime observation during
107 clear sky conditions. Typical compatibility (uncorrected bias) of the EM27/SUN retrievals of
108 the different instruments in a local network is better than 0.01 % (i.e. ` 0.04 ppm) after a careful
109 calibration procedure and a harmonized processing scheme for all spectrometers [[Frey et al.](#)
110 [2015](#)]. The Collaborative Carbon Column Observing Network (COCCON) [[Frey et al. 2018](#)]
111 intends to offer such a framework for operating the EM27/SUN. This type of spectrometer

Formatted: Superscript

112 therefore represents a remarkable opportunity to document XCO₂ variability in cities as a direct
113 way to estimate FFCO₂ [Hase et al. 2015] or in preparation of satellite missions.

114 When future low-Earth-orbit operational satellites with imaging passive spectrometers of
115 suitable capabilities to invert FFCO₂ will sample different cities, this will likely be limited to clear
116 sky conditions and at a time of the day close to local noon. Increasing the density of the
117 COCCON network stations around cities will allow to evaluate those XCO₂ measurements and
118 to monitor XCO₂ during the early morning and afternoon periods, ~~which will not be sampled~~
119 ~~with satellites low-earth orbit satellite, ~~except f~~From geostationary orbit, which can also have~~
120 ~~other benefits, those time-periods can however be observed and could be compared to~~
121 ~~ground-based measurements [e.g. Butz et al., 2015, O'Brien et al. 2016].~~

122 This study focuses on the measurements of XCO₂ from ground based EM27/SUN
123 spectrometers deployed within the Paris metropolitan area during a field campaign in the
124 spring of 2015, and modelling results. This campaign can be seen as a demonstration of the
125 COCCON network concept applied to the quantification of an urban FFCO₂ source. Several
126 spectrometers were operated by different research groups, while closely following the
127 common procedures suggested by Frey et al. [2015]. The paper is organised as follows. After
128 the instrumental and modelling setup descriptions of section 2, the observations of the field
129 campaign and the modelling results will be presented in section 3. Results are discussed in
130 section 4 together with the study conclusions.

131

132 **2 Methods and materials**

133 **2.1 Description of study area and field campaign design**

134 During the COCCON field campaign (April 28th to May 13th, 2015) five portable FTIR
135 spectrometers (EM27/SUN, Bruker Optik, Karlsruhe, Germany) were deployed in the Parisian
136 region (administratively known as *Île-de-France*) and within the city of Paris. The campaign
137 was conducted in early spring as the cloud cover is typically low in April and May and the time
138 between sunrise and sunset is more than 14 hours.

139 The Paris metropolitan area houses over 12 million people, with about 2.2 million inhabiting
140 the city of Paris. This urban region is the most densely populated in France with ~1000
141 inhabitants/km² and over 21000 inhabitants/km² for the city of Paris itself [INSEE 2016 -
142 <https://www.insee.fr/fr/statistiques>]. The estimated CO₂ emissions from the metropolitan
143 region are 39 Mt/year, according to the air quality association (AIRPARIF), that monitors the
144 airshed of Greater Paris, with on-road traffic emissions, and residential and the tertiary (i.e.
145 commercial) sector ~~as~~ are the main sources (accounting for over 75 %), and minor
146 contributions from other sectors such as industrial sources and airports [~~AIRPARIF~~
147 <https://www.airparif.asso.fr/en/>, AIRPARIF 2016]. It was crucial to understand the spatial
148 distribution of these CO₂ sources to optimally deploy the COCCON spectrometers. To this end

149 a 1 km emission model for France by IER (Institut fuer Energiewirtschaft und Rationelle
150 Energieanwendung, University of Stuttgart, Germany) was used as a starting point [Latoska
151 2009]. This emission inventory is based on the available activity data such as, e.g., traffic
152 counts, housing statistics, or energy use, and the temporal disaggregation was implemented
153 according to Vogel et al. [2013]. In brief, the total emissions of the IER model were re-scaled
154 to match the temporal factors for the different emission sectors according to known national
155 temporal emission profiles.

156 To quantify the impact of urban emissions on XCO₂, the FTIR instruments were deployed
157 along the dominant wind directions in this region in spring, i.e., southwesterly [Staufer et al
158 2016], in order to maximize the likelihood to capture upwind and downwind air masses (see
159 Figure 1). The two southwesterly sites (GIF and RES) are located in a less densely populated
160 area, where emissions are typically lower than in the city centre, where the station JUS is
161 located. The data in Fig. 1 show that the densest FFCO₂ emission area extends northwards
162 and eastwards. The two Northwesterly sites (PIS and MIT) were placed downwind of this area.
163 All instruments were operated manually and typically started ~~for~~ operations around 7-8 am
164 local time from which they continuously observe XCO₂ until 5-6 pm.

165

166 2.2 Instrumentation, calibration, and data processing

167 The EM27/SUN is a portable FTIR spectrometer which has been described in detail in, e.g.,
168 Gisi et al. [2012] and Frey et al. [2015]. Here, only a short overview is given. The centre piece
169 of the instrument is a Michelson interferometer which splits up the incoming solar radiation
170 into two beams. After inserting a path difference between the beams, the partial beams are
171 recombined. The modulated signal is detected by an InGaAs detector covering the spectral
172 domain from 5000 to 11000 cm⁻¹ and is called an interferogram. As the EM27/SUN analyzes
173 solar radiation, it can only operate in daylight sunny conditions. A Fourier transform of the
174 interferogram generates the spectrum and a DC correction is applied to remove the
175 background signal and only keep the AC signal (see Keppel-Aleks et al. [2007]). A numerical
176 fitting procedure (PROFFIT code) [Schneider and Hase et al., 2009] then retrieves column
177 abundances of the concentrations of the observed gases from the spectrum. The single-
178 channel EM27/SUN is able to measure total columns of O₂, CO₂, CH₄ and H₂O. The ratio over
179 the observed O₂ column, assumed to be known and constant, delivers the column-averaged
180 trace gas concentrations of XCO₂, XCH₄ in μmol / mol dry air, with a temporal resolution of
181 one minute. XCO₂ is the dry air mole fraction of CO₂, defined as $XCO_2 = \text{Column}[CO_2] /$
182 $\text{Column}[\text{Dry Air}]$. Applying the ratio over the observed oxygen (O₂) column reduces the effect
183 of various possible systematic errors; see Wunch et al. (2011).

184 In order to correctly quantify small differences in XCO₂ columns between Paris city upstream
185 and downstream locations, measurements were performed with the five FTIR instruments side

Formatted: Subscript

186 by side before and after the campaign, as we expect small calibration differences between the
187 different instruments due to slightly different alignment for each individual spectrometer. These
188 differences are constant over time and can be easily accounted for by applying a calibration
189 factor for each instrument. Previous studies showed that the instrument specific corrections
190 are well below 0.1 % for XCO₂ [Frey et al. 2015, Chen et al. 2016] and are stable for individual
191 devices. The 1-sigma precision for XCO₂ is in the order of 0.01 % - 0.02 % (< 0.08 ppm) e. g.
192 [Gisi et al. 2012, Chen et al. 2016, Hedelius et al. 2016, Klappenbach et al. 2015]. The
193 calibration measurements for this campaign were performed in Karlsruhe w.r.t. the Total
194 Carbon Column Observing Network (TCCON) [Wunch et al. 2011] spectrometer at the
195 Karlsruhe Institute of Technology (KIT), Germany –for 7 days before the Paris campaign
196 between April 9th and 23rd, and after the campaign on May 18th until 21st.

197 Figure 2-S1 (left panel) shows the XCO₂ time series of the calibration campaign, where small
198 offsets between the instruments raw data are visible. As these offsets are constant over time,
199 a calibration factor for each instrument can be easily applied; actually these are the calibration
200 factors previously found for the Berlin campaign [Frey et al. 2015]. These factors are given in
201 Table 21, where all EM27/SUN instruments are scaled to match instrument No. 1. The
202 calibrated XCO₂ values for April 15th are shown in Fig. 2-S1 (right panel). None of the five
203 instruments that participated in the Berlin campaign show any significant drift; in other words,
204 the calibration factors found one year before were still applicable. This is an impressive good
205 demonstration of the instrument stability stated in section 2.2, especially as several
206 instruments (Nos. 1, 3, 5) were used in another campaign in Northern Germany in the
207 meantime. The EM27/SUN XCO₂ measurements can also be made traceable to the WMO
208 international scale for in-situ measurements by comparison with measurements of a collocated
209 TCCON spectrometer from the TCCON. TCCON instruments which are calibrated against in-
210 situ standards by aircraft and aircore measurements [Wunch et al. 2010, Messerschmidt et al.
211 2012] performed using the WMO scale.

212 During the campaign and for the calibration measurements we recorded double-sided
213 interferograms with 0.5 cm⁻¹ spectral resolution. Each measurement of 58 s duration consisted
214 of 10 scans using a scanner velocity of 10 kHz. For precise timekeeping, we used GPS
215 sensors for each spectrometer.

216 In-situ surface pressure data used for the analysis of the calibration measurements performed
217 at KIT have been recorded at the co-located meteorological tall tower. During the campaign,
218 a MHD-382SD data-logger recorded local pressure, temperature and relative humidity at each
219 station. The analysis of the trace gases from the measured spectra for the calibration
220 measurements has been performed as described by Frey et al. [2015]. For the campaign
221 measurements we assume a common vertical pressure-temperature profile for all sites,
222 provided by the model, so that the surface pressure at each spectrometer only differs due to

223 different site altitudes. The 3-hourly temperature profile from the European Centre for Medium-
224 Range Weather Forecasts (ECMWF) operational analyses interpolated for site JUS located in
225 the centre of the array was used for the spectra analysis at all sites. The individual ground-
226 pressure was derived from site altitudes and pressure measurements performed at each site.
227 Before and after the Paris campaign, side by side comparison measurements were performed
228 with all 5 EM27/SUN spectrometers and the TCCON spectrometer operated in Karlsruhe at
229 KIT. All spectrometers were placed on the top of the IMK office building North of Karlsruhe.
230 The altitude is 133 m above sea level (a.s.l.), coordinates are 49.09° N and 8.43° E. The
231 processing of the Paris raw observations (measured interferograms) were performed as
232 described by Gisi et al. [2012] and Frey et al. [2015] for the Berlin campaign: spectra were
233 generated applying a DC correction, a Norton-Beer medium apodization function and a
234 spectral resampling of the sampling grid resulting from the FFT on a minimally sampled
235 spectral grid. PROFFWD was used as the radiative transfer model and PROFFIT as the
236 retrieval code.

237

238 **2.3 Atmospheric transport modelling framework**

239 We used the chemistry transport model CHIMERE (Menut et al., 2013) to simulate CO₂
240 concentrations in the Paris area. More specifically, we used the CHIMERE configuration over
241 which the inversion system of Bréon et al. [2015] and Staufer et al. [2016] was built to derive
242 monthly to 6-hour mean estimates of the CO₂ Paris emissions. Its horizontal grid, and thus its
243 domain and its spatial resolution, are illustrated in Figure S23. It has a 2 × 2 km² spatial
244 resolution for the Paris region, and 2 × 10 km² and 10 × 10 km² spatial resolutions for the
245 surroundings. It has 20 vertical hybrid pressure-sigma (terrain- following) layers that range
246 from the surface to the mid-troposphere, up to 500 hPa. It is driven by operational
247 meteorological analyses of the ECMWF Integrated Forecasting System, available at an
248 approximately 15 × 15 km² spatial resolution and 3 h temporal resolution.

249 In this study the CO₂ simulations are based on a forward run over April 25th - May 12th 2015
250 with this model configuration; we do not assimilate atmospheric CO₂ data and so no inversion
251 for surface fluxes was conducted. In the Paris area (the Île-de-France administrative region),
252 hourly anthropogenic emissions are given by the IER inventory, see section 2.1. The
253 anthropogenic emissions in the rest of the domain are prescribed from the EDGAR V4.2
254 database for the year 2010 at 0.1° resolution [Olivier and Janssens-Maenhout et al., 2012]. In
255 the whole simulation domain, the natural fluxes (the Net Ecosystem Exchange: NEE) are
256 prescribed using simulations of C-TESSSEL, which is the land-surface component of the
257 ECMWF forecasting system [Boussetta et al., 2013], at a 3 hourly and 15 × 15 km² resolution.
258 Finally, the CO₂ boundary conditions at the lateral and top boundaries of the simulation domain
259 and the simulation CO₂ initial conditions on April 25th 2015 are prescribed using the CO₂

Formatted: Subscript

260 forecast issued by the Copernicus Atmosphere Monitoring Service (CAMS,
261 <http://atmosphere.copernicus.eu/>) at a ~15 km global resolution [Agustí-Panareda et al.,
262 2014].

263 The CHIMERE transport model is used to simulate the XCO₂ data. However, since the model
264 does not cover the atmosphere up to its top, the CO₂ fields from CHIMERE are complemented
265 with that of the CAMS CO₂ forecasts from 500 hPa to the top of the atmosphere to derive total
266 column concentrations. The derivation of modelled XCO₂ at the sites, involves obtaining a
267 kernel-smoothed CO₂ profile of CHIMERE and CAMS and vertical integration of these
268 smoothed profiles, weighted by the pressure at the horizontal location of the sites.

269 The parametrisation used to smooth modelled CO₂ profiles approximates the sensitivity of the
270 EM27/sun CO₂ retrieval is a function of pressure and sun elevation. Between 1000 hPa and
271 480 hPa, a linear dependency of the instrument averaging kernels on solar zenith angle (θ) is
272 assumed with boundary values following Frey et al. [2015]:

273

$$274 \quad (1a) \quad k(480 \text{ hPa}) = 1.125$$

$$275 \quad (1b) \quad k(1000 \text{ hPa}) = 1.0 + 0.45 s^3$$

276

277 where $s = \theta/90^\circ$. Approximate averaging kernels are obtained by linear interpolation to the
278 pressure levels of CHIMERE and CAMS, respectively. If $p > 1000$ hPa, k is linearly
279 extrapolated. Above 480 hPa ($p < 480$ hPa), the averaging kernels can be approximated by

280

$$281 \quad (2) \quad k(u, s) = 1.125 - 0.6 u^3 - 0.4 u s^3$$

282

283 where u is $(480 \text{ hPa} - p) / 480$. The kernel-smoothed CO₂ profile, $CO_{2_model}^s$, is obtained by

284

$$285 \quad (3) \quad CO_{2_model}^s = \mathbf{K} CO_{2_model} + (\mathbf{I} - \mathbf{K}) CO_2^a$$

286

287

288 where CO_{2_model} is the modelled CO₂ profile by CHIMERE or CAMS, \mathbf{I} the identity matrix and
289 \mathbf{K} is a diagonal matrix containing the averaging kernels k . The a priori CO₂ profile, CO_2^a , is
290 provided by the Whole Atmosphere Community Climate Model (WACCM) model (version 6)
291 and interpolated to the pressure levels of CHIMERE and CAMS. $CO_{2_model}^s$ is the appropriate
292 CO₂ profile to calculate modelled XCO₂ at the location of the sites.

293

294 For a given site, the simulated XCO₂ data are thus computed from the vertical profile of this
295 site as:

Formatted: Subscript

Formatted: Font: Not Bold

Formatted: Subscript

Formatted: Subscript

296

$$297 \quad (3) \quad XCO_{2_CHIMERE} = \frac{1}{p_{surf}} \int_{p_{surf}}^{p_{top_CHIM}} CO_{2_CHIM}^s dp + \int_{p_{top_CHIM}}^{p=0mbar} CO_{2_CAMS}^s dp$$

298

299 where p_{surf} is the surface pressure, $p_{top_CHIM} = 500$ hPa the pressure corresponding to the top
300 boundary of the CHIMERE model, and $CO_{2_CHIM}^s$ and $CO_{2_CAMS}^s$ are the smoothed CO_2
301 concentrations of CHIMERE and CAMS respectively. For comparison we also calculated
302 XCO_2 at a lower spatial resolution with the CAMS data alone as:

303

$$304 \quad (4) \quad XCO_{2_CAMS} = \int_{p_{surf}}^{p=0mbar} CO_{2_CAMS}^s dp$$

305

306 **3 Results and discussion**

307 **3.1 Observations**

308 **3.1.1 Meteorological conditions and data coverage/instrument performance.**

309 During the measurement campaign (April 28th until May 13th, 2015), meteorological conditions
310 were a major limitation for the availability of XCO_2 observations. Useful EM27/SUN
311 measurements require direct sunlight and low wind speeds typically yield higher local XCO_2 .
312 Most of the time during the campaign conditions were partly cloudy and turbid, and so
313 successful measurements at high solar zenith angle (SZA) were rare. Therefore, the data
314 coverage between April 28th and May 3rd is limited (see Table 32). As is typical for spring
315 periods in Paris, the temperature and the wind direction vary and display less synoptic
316 variations than in winter. The dominant wind directions were mostly northeasterly at the
317 beginning of the campaign and mostly southeasterly during the second half of the campaign.
318 We find that the wind speeds during daytime nearly always surpass 3 m s^{-1} , which has been
319 identified by Breon et al. [2015] and Staufer et al. [2016] as the cut-off wind speed above which
320 the atmospheric transport model CHIMERE performs best in modelling CO_2 concentration
321 gradients in the mixed layer.

322 Despite some periods with unfavourable conditions, more than 10,000 spectra were retrieved
323 among the five deployed instruments. The quality of the spectra for each day was rated
324 according to the overall data availability and consistent with Hase et al. (2015). The best
325 measurement conditions prevailed for the period between May 7th and May 12th.

326

327 **3.1.2 Observations of XCO_2 in Paris**

328 The observed XCO_2 in the Paris region for all sites (10415 observations) ranges from 397.27
329 to 404.66 ppm with a mean of 401.26 ppm (a median of 401.15 ppm). The strong atmospheric
330 variability of XCO_2 across Paris and within the campaign period is reflected in the and a
331 standard deviation of 1.04 ppm for 1-minute averages. We find that all sites exhibit very similar

Formatted: Subscript

332 diurnal behaviours with a clear decrease of XCO₂ during daytime and a noticeable day-to-
333 day variability as seen in Figure 42. This is to be expected as they are all subject to very similar
334 atmospheric transport in the boundary layer height and to similar large-scale influences, i.e.,
335 surrounding with stronger natural fluxes or air mass exchange with other regions at synoptic
336 time scales. However, observed XCO₂ concentrations at the ~~upwind-downwind~~ sites for our
337 network remain clearly higher from sites that are ~~downwind-upwind~~ of Paris (see Figure
338 42). ~~The shifting dominant wind conditions also explain why the site RES and GIF are lowest~~
339 ~~in the beginning of the campaign and higher on May 12th and 13th after meteorological~~
340 ~~conditions changed.~~ This indicates that the influence of urban emissions is detectable with this
341 network configuration under favourable meteorological conditions. By comparing the different
342 daily variations in Fig. 53, it is apparent that the day-to-day variations observed at the two
343 southwesterly (typically upwind) sites GIF and RES are approximately 1 ppm, with both sites
344 exhibiting similar diurnal variations throughout the campaign period. This can be expected as
345 their close vicinity would suggest that they are sensitive to emissions from similar areas and
346 to concentrations of air masses arriving from the southwest.

347 The typical decrease in XCO₂ found over the course of a day is about 2 to 3 ppm. This
348 decrease ~~can-could only~~ be driven by (natural) sinks of CO₂, which can be expected to be very
349 strong as our campaign took place after the start of the growing season in Europe for most of
350 southern and central Europe [Roetzer and Chmielewski 2001].

351 The observations at the site located in Paris (JUS) displays similarly low day-to-day variations
352 and a clear decrease in XCO₂ over the course of the day. The latter feature indicates that even
353 in the dense city centre, XCO₂ is primarily representative of a large footprint like in other areas
354 of the globe [Keppel-Aleks 2011] and supports the findings of [Keppel-Aleks, 2014; Belikov et
355 al. (2017)] concerning the footprints for the Paris and Orleans TCCON sites. Thus, our total
356 column ~~-and is not as~~ observations are less critically affected by local emissions than in-situ
357 measurements [Breon et al. 2015, Ammoura et al. 2016]. It is also apparent that the decrease
358 in XCO₂ (the slope) during the afternoon for April 28th and 29th as well as May 7th and 10th is
359 noticeably smaller than at other days during this campaign. As XCO₂ is not sensitive to vertical
360 mixing, this has to be caused by different CO₂ sources and sinks acting upon the total column
361 arriving at JUS.

362 The two ~~northeasterly~~ (typically downwind) sites PIS and MIT northeast of Paris show a
363 markedly larger day-to-day spread in ~~the their general XCO₂ levels-background~~ as well as
364 strongly changing slopes for the diurnal XCO₂ decrease. For these sites the exact wind
365 direction is critical as they can be downwind of the city centre that has a much higher emission
366 density or less dense suburbs (see Fig. 1).

367 3.1.3 Gradients in observed XCO₂

Formatted: Superscript

Formatted: Superscript

Formatted: Subscript

369 In order to focus more on the impact of local emissions on atmospheric conditions and less on
370 that of ~~background of CO₂ fluxes from outside of our urban domain influences~~ in our analysis
371 of XCO₂, we choose to study the spatial gradients (Δ) between different sites. Fundamentally,
372 this approach assumes that regional and large-scale fluxes have a similar impact on XCO₂ for
373 the sites within our network, due to the close proximity of sites and the smoothing of remote
374 emission signals due to atmospheric transport by the time the air-mass arrives in our domain.
375 Ideal conditions were sampled during May 7th, with predominantly southwesterly winds, and
376 on May 10th with southerly winds. We can see in Fig. ~~6-4~~ that all sites ~~were~~are, on average,
377 elevated compared to RES, chosen as reference here as it was upwind of Paris during ~~the~~
378 ~~measurement period~~those days. The hodographs for both days also indicate that the wind
379 fields were consistent across Paris (see Figure S3). -The observations from GIF ~~only~~showed
380 only minimal differences with RES, while the rest of the sites (PIS, JUS and MIT) ~~an~~ had Δ
381 values of increases between PIS, JUS and MIT and RES to reach 1 to 1.5 ppm. During
382 southwesterly winds, MIT is downwind ~~of most~~ of the densest part of the Paris urban area,
383 and JUS is impacted by emissions of neighborhoods to the southwest. The site of PIS is still
384 noticeably influenced by the city centre but, as can be seen in Fig. 1, we likely do not catch
385 the plume of the most intense emissions but rather from the suburbs. On May 10th, with its
386 dominant southerly winds, the situation ~~is~~was markedly different. While GIF ~~was~~is still only
387 slightly elevated, the XCO₂ enhancement at MIT ~~is~~was significantly lower and quite similar to
388 JUS for large parts of the day. The highest Δ XCO₂ can ~~now~~be observed at PIS, again typically
389 ranging from 1 to 1.5 ppm. As seen in Fig. 1, PIS is ~~now~~then directly downwind of the densest
390 emission area, while MIT is only exposed to CO₂ emissions from the eastern outskirts of Paris.
391 It is also important to note that the impact of the local biosphere that is assumed to cause the
392 strong decrease in XCO₂ during the day is not seen on both days for these spatial gradients.
393 For a more comprehensive interpretation of these observations the use of a transport model
394 (as described in section 2.3) is necessary.

Formatted: Subscript

Formatted: Subscript

395

396 3.2 Modelling

397 3.2.1 Model performance

398 Before interpreting the modelled XCO₂ we need to evaluate the performance of the chosen
399 atmospheric transport model framework as described in section 2.3. Comparing it to
400 meteorological observations (wind speed and wind direction) at GIF ~~in Fig. 7~~, we find that
401 CHIMERE predicts these variables well throughout the duration of the campaign (see Figure
402 S4). Changes in wind speed direction and speed are reproduced with a slight overestimation
403 at low wind-speeds (>1m/s). Besides the meteorological forcing, the model performance can
404 also be expected to depend on the chosen model resolution. Therefore, we compared XCO₂
405 at JUS calculated based on the coarser resolution atmospheric transport and flux framework

406 CAMS (15 km), and the higher resolution emission modelling input for the framework based
407 on CHIMERE (2 km) for the inner domain and on CAMS boundary conditions (see Fig. S29).
408 We find that the coarser model displays similar inter-daily variations, but that the high-
409 resolution model modifies the modelling results on shorter time-scales. We find that the
410 afternoon XCO₂ decreases are often more pronounced in CHIMERE. Only the high-resolution
411 will be considered and referred to in the following.

412
413 The impact of using different flux maps (fossil fuel CO₂ ~~and biosphere models~~) on the modelled
414 XCO₂ can unfortunately not be explicitly investigated here as only one high-resolution (1 km)
415 emission product available for fossil fuel CO₂ was available for this study region (see section
416 2.3) and other global emission products are usually not intended for urban-scale studies.

Formatted: Subscript

417

418 3.2.2 Modelled XCO₂ and its components

419 The modelled XCO₂ for the five sites (Fig. 95) co-evolves over the period of the campaign with
420 occurrences of significant differences. This was already seen with the measurements, but the
421 model allows looking at the full time series. The model reveals clear daily cycles of XCO₂, with
422 an accumulation during night-time and a decrease during daytime. Despite a good general
423 agreement of modelled XCO₂ at all sites for, e.g., the timing of daily minima and their synoptic
424 changes, differences in XCO₂ are observed between the sites for many days. Typically the
425 northeasterly sites (PIS, MIT) show an enhancement in modelled XCO₂ compared to the
426 southwesterly sites (GIF, RES).

427 To understand the synoptic and diurnal variations of the modelled XCO₂, we analyzed the
428 contribution of different sources (and sinks) of CO₂, namely the net ecosystem exchange
429 (NEE), the fossil fuel CO₂ emissions (FFCO₂), and the boundary conditions (BC), i.e., the
430 variations of CO₂ not caused by fluxes within our domain (the example of JUS is given in Fig.
431 ~~106; see the supplement for the other sites~~). The day-to-day variability of modelled XCO₂ is
432 dominated by changing boundary conditions and coincides with synoptic weather changes.

433 As the CO₂ emitted from the different sources is transported in the model as independent
434 tracers, ~~The~~ the strong daily decrease in XCO₂ can be directly linked to NEE, which leads to a
435 decrease of ~1 ppm (but up to 4 ppm) during the day, but can also cause positive
436 enhancements during nighttime driven by biogenic respiration. The XCO₂ from fossil fuel
437 emissions causes significant enhancements compared to the background, but is often
438 compensated by NEE. During short periods, fossil fuel emissions can however lead to
439 enhancements of up to 4 ppm.

Formatted: Subscript

440

441 3.2.3 Modelled ΔXCO₂ gradients and its components

442 To be able to assess the impact of local sources and reduce the influence of NEE and BC on
443 the modelled signals, we analyse the XCO₂ gradient (i.e. station-to-station difference) with
444 RES being taken as reference. In Fig. 41-7 we compare Δ in the top panel, and its
445 components, i.e. fossil fuel CO₂, biogenic CO₂ and CO₂ transported across the boundary of
446 the domain (boundary conditions: BC), along a south-north direction. For the modelled Δ we
447 can see that MIT shows a positive value during the campaign period whenever the
448 predominant wind direction was southwesterly (grey shaded areas). We also find that Δ
449 between JUS and RES was both negative and positive during the campaign, and
450 predominantly negative between MIT and JUS. When split into FFCO₂, BC and NEE
451 components, we can clearly see that the total Δ is dominated by FF causing XCO₂ offsets of
452 up to 4 ppm, but more typically 1 ppm gradients are observed. Gradients can also change
453 rapidly (within a few hours) if the wind direction changes, for example on May 1st and May 12th.
454 This highlights the fact that, during such conditions, we cannot assume a simple upwind-
455 downwind interpretation of our sites. As expected, the contributions from BC and NEE are
456 generally greatly reduced when analysing Δ XCO₂. The most important impact of NEE on the
457 XCO₂ gradients of -1ppm and +1ppm can be seen on May 8th and May 11th, respectively. This
458 means that, despite greatly reducing the impact of NEE on average, the contribution of NEE
459 cannot be fully ignored. BC is an overall negligible contribution to Δ XCO₂, even though it
460 reaches -0.4 ppm on May 11th.

461

462 3.3 Model data and observations comparison

463 3.3.1 XCO₂

464 A comparison of modelled and observed XCO₂ is of course limited to the relatively short
465 periods when observations are available. Over these periods ~~We can also see a general~~
466 ~~issue in reproducing the background~~ general XCO₂ for each day in the model as observed
467 ~~XCO₂ is significantly lower by typically~~ revealing a fairly stable bias between 1 to 2 ppm. As our
468 ~~CO₂ boundary conditions were from a forecast product, this is not unexpected, as already~~
469 ~~small issues in estimating carbon uptake (or emissions) at the European scale can have such~~
470 ~~an impact on the boundary conditions. However,~~ we observe that the main features, like daily
471 ~~cycles and synoptic changes~~ of the modelled and observed XCO₂ are comparable as seen in
472 Figure 8. The daytime variations are well reproduced by the model and the general relative
473 concentrations between sites are preserved, e.g., the highest values for XCO₂ at MIT are on
474 May 9th and highest XCO₂ for PIS are later on May 10th and May 11th as seen in Figure 12.
475 ~~We can also see a general issue in reproducing the background XCO₂ for each day in the~~
476 ~~model as observed XCO₂ is significantly lower by typically between 1 to 2 ppm.~~ We also see
477 that the timing of the daily minima is not fully covered in the observed data as it typically

Formatted: Subscript

Formatted: Subscript

Formatted: Subscript

Formatted: Subscript

478 happens after sunset and cessation of biosphere uptake. To reduce the impact of uncertainties
479 of the boundary conditions on our analysis a gradient approach was tested.

480

481 3.3.2 ΔXCO_2

482 Due to the prevailing southeasterly wind conditions, we can compare XCO_2 at the typical
483 downwind sites (PIS, MIT) relative to the mostly upwind sites (RES, GIF) and expect elevated
484 XCO_2 downwind. Furthermore, we can expect to see negative gradients for opposing wind
485 conditions, i.e. northwesterly. For other wind conditions, the concentration difference is not
486 determined by emissions between the station pairs, but rather by the areas upwind of the sites.
487 (see Figure 1). We find that the ΔXCO_2 of PIS relative to RES generally falls along the 1:1 line
488 with a slope of 1.07 ± 0.09 with a Pearson's R of 0.8. Negative ΔXCO_2 values, seen in Fig. 439,
489 are associated with meteorological conditions when winds come from northerly ~~or easterly~~
490 directions, i.e., the roles of normal upwind and downwind sites are reversed. For wind
491 perpendicular to the direct line of sight for (PIS, RES) the concentration enhancements are
492 small and harder to interpret and no slope was calculated. The gradient of XCO_2 MIT relative
493 to RES has a significantly lower range for modelled XCO_2 while the observed range of XCO_2
494 is similar to PIS. The slope of observed to modelled ΔXCO_2 for upwind-downwind (or
495 downwind-upwind conditions) is 1.72 ± 0.06 with a Pearson's R of 0.96. This points to a
496 significant underestimation of the impact of urban sources on the MIT-RES gradient, which is
497 ~~also especially~~ visible in the more negative ΔXCO_2 during northerly wind conditions. This could
498 indicate that the spatial distribution of our emissions prior should be improved, i.e., emissions
499 in the eastern outskirts/suburbs are likely underestimated in the IER emissions model. The
500 low modelled ΔXCO_2 could also be due to overestimated horizontal dispersion in the model,
501 which seems less likely. Again the model does not predict concentration differences well for
502 perpendicular wind conditions. When comparing the mean modelled daily cycle of the days
503 with south-westerly wind conditions and when observations exist with the mean diurnal cycle
504 for all days within the field campaign period when MIT and PIS can be considered downwind
505 of RES, we find that the days with observations do not significantly differ from those without
506 observations (see Fig. 4410). An investigation of typical diurnal variations of modelled ΔXCO_2
507 can only be performed to a limited degree with the observational data available for suitable
508 wind conditions. Within the large uncertainties, the modelled and observed ΔXCO_2 agree
509 throughout the day. When analysing the modelled ΔXCO_2 components we also find that the
510 observed daytime increases of ΔXCO_2 are driven by CO_2 added by urban FF CO_2 burning
511 and that the impact of FF is significantly higher at PIS (up to 1 ppm) than at MIT site (0.5 ppm)
512 in the model. when both sites are downwind of Parisian emissions. Our observations indicate
513 that both sites have strong diurnal variations. ~~As~~ Given that the most important biogenic sinks,

514 ~~in our domain, can be expected to be found in the rural parts surrounding Paris we would~~
515 ~~expect~~ the biogenic contribution ~~is expected~~ to be similar ~~at both sites (as predicted by the~~
516 ~~model-). this-This is another~~would further point towards, ~~indication~~ that the impact of FF
517 emissions on the MIT site is larger than predicted by our modelling framework.

518 Different ΔXCO_2 diurnal variations can be found for other upwind-downwind site pairs, but they
519 are all systematically driven by the locally-added CO_2 from FFCO₂.

520

521 5 Conclusion and Outlook

522 For the two-weeks field campaign we demonstrated the ability of a network of five EM27/SUN
523 spectrometers, placed in the outskirts of Paris, to ~~successfully~~ track the XCO_2 changes due
524 to the urban plume of the city. However, we also found that XCO_2 cannot be ~~simply interpreted~~
525 ~~in the context of local emission~~~~easily linked to local emissions~~ as, even in such a densely
526 populated area, XCO_2 is still significantly influenced by natural CO_2 uptake during the growing
527 season. ~~Understanding the area influencing XCO_2 and/or the use of suitable atmospheric~~
528 ~~transport models seems indispensable to correctly interpret atmospheric XCO_2 variations.~~

Formatted: Subscript

Formatted: Subscript

529 Using a gradient approach, i.e., analysing the difference between XCO_2 measured at upwind
530 and downwind stations, greatly reduced the impact of ~~remote- CO_2 sinks~~~~boundary condition,~~
531 ~~that reflect fluxes outside the domain and biogenic fluxes within the domain.~~ Overall, the XCO_2
532 variability modelled using our ECMWF-CHIMERE system with IER (1 x 1 km²) emissions data
533 was found to be comparable with the observed variability and diurnal evolution of XCO_2 ,
534 despite a ~~significantly enhanced~~~~higher~~ background for modelled XCO_2 . Our modelling
535 framework, run at a 2 x 2 km² resolution over Paris also predicts that ~~NEE-biogenic fluxes~~ and
536 ~~boundary conditions (i.e. the influence of CO_2 being transported into our domain)~~~~BC~~ ~~have only~~
537 ~~very small impact on ΔXCO_2~~ only ~~significantly-noticeably impacts~~~~impacting it~~ ΔXCO_2 during a

Formatted: Subscript

538 few situations, specifically when meteorological conditions changes ~~making-made~~ the concept
539 of 'upwind' and 'downwind' not applicable. When comparing modelled and measured ΔXCO_2
540 we find strong correlations (Pearson's R) of 0.8 and 0.96 for PIS-RES and MIT-RES,
541 respectively. ~~This can be considered as an excellent degree of correlation as even a model~~
542 ~~simulation which used optimised fluxes, based on surface observation, showed correlations~~
543 ~~of 0.91 for its posterior results [Breon et al. 2015].~~ The offset between model and observations
544 also diminished for ΔXCO_2 and the slope found between observed and modeled PIS-RES
545 gradient is statistically in accordance with a 1:1 relationship (1.07±0.09). However, the slope
546 of the MIT-RES XCO_2 gradient of 1.72±0.06 suggests that the emission model could
547 potentially be improved, ~~as it seems unlikely that the general atmospheric transport in the~~
548 ~~model is the key issue as both site pairs would be subject to very similar winds.~~ Another
549 ~~potential source of error that needs to be investigated is~~ ~~unless this~~if such an underestimation

550 of ΔXCO_2 ~~could be caused by the limited model resolution. is caused by overestimated~~
551 ~~dispersion in the model.~~ It also seems rather likely that ~~a 2x2km² model the dispersion~~ would
552 cause a general spreading of ~~emission plumes point source emissions~~ and not systematically
553 underestimate emissions impacts from less densely populated, parts of Île-de-France. The
554 data also confirm previous results by models that XCO_2 gradients caused by a megacity do
555 not exceed 2 ppm, which supports the previous requirement for satellite observations of less
556 than 1 ppm precision on individual soundings, and biases lower than 0.5 ppm (Ciais et al.
557 2015). The gradients are mainly caused by the transport of FFCO₂ emissions but, interestingly,
558 during specific episodes, a ~~significant noticeable~~ contribution comes from biogenic fluxes,
559 suggesting that these fluxes cannot always be neglected even when using gradients.
560 Unfortunately, the duration of the campaign was relatively short, so that an in-depth analysis
561 of mean daily cycles or the impact of ambient conditions (traffic conditions, temperature, solar
562 insolation, etc.) on the observed gradient and underlying fluxes could not be investigated here.
563 Hence, future studies in Paris and elsewhere should aim to perform longer-term observations
564 during different seasons, which will allow better understanding changes in biogenic and
565 anthropogenic CO₂ fluxes. A remotely-controllable shelter for the EM27/SUN instrument is
566 currently under development [Heinle and Chen, 2017]. This will considerably facilitate the
567 establishment of permanent spectrometer arrays around cities and other sources of interest.
568 Nevertheless, our study already indicates that such observations of urban XCO_2 and ΔXCO_2
569 contain original information to understand local sources and sinks and that the modelling
570 framework used here is ~~suitable a step forward~~ to support their detailed interpretation in the
571 future. An improved model will also be able to adjust or better model the background conditions
572 and potentially use this type of observations to estimate local CO₂ fluxes using a Bayesian
573 inversion scheme similar to the existing system based on in-situ observations for Paris [Staufer
574 et al. 2016].
575 We expect that the previous successful collaboration in the framework of the Paris campaign
576 will mark the permanent implementation of COCCON as a common framework for a French-
577 Canadian-German collaboration on the EM27/SUN instrument. The acquisition of additional
578 spectrometers is planned by several partners.

579 **Author contribution**
580 FRV, MF, FH, IXR, MKS, PCh, PJ, YVT, CJ, TB, QT and JO, supported the field campaign
581 and contributed data to this study.
582 MF, FH, FRV, JS, GB and PCi planned the fieldwork and modelling activities for this study.
583 JS, GB, FC, and FRV performed the CHIMERE modelling, provided modelling data input
584 and/or analysed the output data.

Formatted: Superscript

586 MF, FH and FRV processed and analysed the EM27Sun data.
587 FRV, MF, JS, FH and PCi wrote sections of the manuscript and created figures and tables.
588 All authors reviewed, edited and approved the manuscript.

589 **Acknowledgement:**

591 All authors would like to thank the two anonymous reviewers for their comments that helped
592 to significantly improve this manuscript. ECCC would like to thank Ray Nasser (CRD) and
593 Yves Rochon (AQRD) for their internal review. The authors from LSCE acknowledge the
594 support of the SATINV group of Frederic Chevallier. The authors from KIT acknowledge
595 support from the Helmholtz Research Infrastructure ACROSS. The authors from LISA
596 acknowledge support from the OSU-EFLUVE (Observatoire des Sciences de l'Univers-
597 Enveloppes Fluides de la Ville à l'Exobiologie).

599 **References**

601 Agustí-Panareda, A., Massart, S., Chevallier, F., Bousetta, S., Balsamo, G., Beljaars, A., Ciais, P.,
602 Deutscher, N.M., Engelen, R., Jones, L. and Kivi, R., 2014. Forecasting global atmospheric CO₂.
603 Atmospheric Chemistry and Physics, 14(21), pp.11959-11983.

604 AIRPARIF, 2016. Inventaire régional des émissions en Île-de-France Année de référence 2012 –
605 éléments synthétiques, Edition Mai 2016, Paris, France. Last access Dec. 14th, 2017, available at:
606 https://www.airparif.asso.fr/_pdf/publications/inventaire-emissions-idf-2012-150121.pdf

607 Ammoura, L., Xueref-Remy, I., Vogel, F., Gros, V., Baudic, A., Bonsang, B., Delmotte, M., Té, Y. and
608 Chevallier, F., 2016. Exploiting stagnant conditions to derive robust emission ratio estimates for CO₂,
609 CO and volatile organic compounds in Paris. Atmospheric Chemistry and Physics, 16(24), pp.15653-
610 15664.

611 Belikov, D., Maksyutov, S., Ganshin, A., Zhuravlev, R., Deutscher, N.M., Wunch, D., Feist, D.G.,

612 Morino, I., Parker, R.J., Strong, K. and Yoshida, Y., 2017. Study of the footprints of short-term
613 variation in XCO₂ observed by TCCON sites using NIES and FLEXPART atmospheric transport
614 models.

615 Bréon, F.M., Broquet, G., Puygrenier, V., Chevallier, F., Xueref-Remy, I., Ramonet, M., Dieudonné, E.,
616 Lopez, M., Schmidt, M., Perrussel, O. and Ciais, P., 2015. An attempt at estimating Paris area CO₂
617 emissions from atmospheric concentration measurements. Atmospheric Chemistry and Physics, 15(4),
618 pp.1707-1724. <https://doi.org/10.5194/acp-15-1707-2015>, 2015.

619 Broquet, G., Bréon, F.M., Renault, E., Buchwitz, M., Reuter, M., Bovensmann, H., Chevallier, F., Wu,
620 L. and Ciais, P., 2018. The potential of satellite spectro-imagery for monitoring CO₂ emissions from
621 large cities. Atmospheric Measurement Techniques, 11(2), pp.681-708.

622 Broquet, G., Bréon, F.M., Renault, E., Buchwitz, M., Reuter, M., Bovensmann, H., Chevallier, F., Wu
623 L., and P. Ciais, 2017 in review. The potential of satellite spectro-imagery for monitoring CO₂ emissions
624 from large cities.

Formatted: French (Canada)

Formatted: English (United States)

Formatted: French (Canada)

Formatted: Font: 10 pt

Formatted: Font: 10 pt

Formatted: Font: 10 pt

Formatted: Font: 10 pt

Formatted: Font: 10 pt

Formatted: Font: 10 pt, Not Italic

Formatted: Font: 10 pt

Formatted: Font: 10 pt, Not Italic

Formatted: Font: 10 pt

Formatted: Font: 10 pt, English (Canada)

625 Boussetta, S., Balsamo, G., Beljaars, A., Panareda, A.A., Calvet, J.C., Jacobs, C., Hurk, B., Viterbo,
626 P., Lafont, S., Dutra, E. and Jarlan, L., 2013. Natural land carbon dioxide exchanges in the ECMWF
627 Integrated Forecasting System: Implementation and offline validation. *Journal of Geophysical*
628 *Research: Atmospheres*, 118(12), pp.5923-5946.

629 Butz, A., Orphal, J., Checa-Garcia, R., Friedl-Vallon, F., von Clarmann, T., Bovensmann, H.,
630 Hasekamp, O., Landgraf, H., Knigge, T., Weise, D., Sqalli-Houssini, O., and D. Kemper, Geostationary
631 Emission Explorer for Europe (G3E): mission concept and initial performance assessment, *Atmos.*
632 *Meas. Tech.*, 8, 4719-4734, 2015

Formatted: Font: 10 pt

633 Chen, J., Viatte, C., Hedelius, J. K., Jones, T., Franklin, J. E., Parker, H., Gottlieb, E. W., Wennberg, P.
634 O., Dubey, M. K., and Wofsy, S. C., 2016. Differential column measurements using compact solar-
635 tracking spectrometers, *Atmos. Chem. Phys.*, 16, 8479-8498, [https://doi.org/10.5194/acp-16-8479-](https://doi.org/10.5194/acp-16-8479-2016)
636 [2016](https://doi.org/10.5194/acp-16-8479-2016), 2016.

637 Ciais, P., Crisp, D., Denier van der Gon, H., Engelen, R., Heimann, M., Janssens-Maenhout, G.,
638 Rayner, P. and Scholze, M., 2015. Towards a European Operational Observing System to Monitor
639 Fossil CO₂ Emissions. Final Report from the Expert Group, European Commission, October 2015.
640 Available at http://edgar.jrc.ec.europa.eu/news_docs/CO2_report_22-10-2015.pdf Accessed February
641 6th, 2018

642 Dhakal, S., 2009. Urban energy use and carbon emissions from cities in China and policy implications,
643 Energy Policy 37:4208-4219

644 Frey, M., F. Hase, T. Blumenstock, J. Groß, M. Kiel, G. Mengistu Tsidu, K. Schäfer, M. Kumar Sha, and
645 J. Orphal, 2015. Calibration and instrumental line shape characterization of a set of portable FTIR
646 spectrometers for detecting greenhouse gas emissions, *Atmos. Meas. Tech.*, 8, 3047-3057,
647 doi:10.5194/amt-8-3047-2015

648 Frey, M., Sha, M.K., Hase, F., Kiel, M., Blumenstock, T., Harig, G., Surawicz, G., Deutscher, N.M.,
649 Shiomi, K., Franklin, J., Bösch, H., Chen, J., Grutter, M., Ohyama, H., Sun, Y., Butz, A., Mengistu Tsidu,
650 G., Ene, D., Wunch, D., Song, C.Z., Garcia, O., Ramonet, M., Vogel, F., and J. Orphal, Building the
651 COllaborative Carbon Column Observing Network (COCCON): Long term stability and ensemble
652 performance of the EM27/SUN Fourier transform spectrometer, *Atmos. Meas. Tech. Diss*, submitted,
653 2018

Formatted: Font: 10 pt

654 Gisi, M., F. Hase, S. Dohe, T. Blumenstock, A. Simon, and A. Keens, 2012. XCO₂-measurements with
655 a tabletop FTS using solar absorption spectroscopy, *Atmos. Meas. Tech.*, 5, 2969-2980,
656 doi:10.5194/amt-5-2969-2012

657 Hase, F., M. Frey, T. Blumenstock, J. Groß, M. Kiel, R. Kohlhepp, G. Mengistu Tsidu, K. Schäfer, M. K.
658 Sha, and J. Orphal, 2015. Application of portable FTIR spectrometers for detecting greenhouse gas
659 emissions of the major city Berlin, *Atmos. Meas. Tech.*, 8, 3059-3068, doi:10.5194/amt-8-3059-2015

660 Hase, F., M. Frey, M. Kiel, T. Blumenstock, R. Harig, A. Keens, and J. Orphal, 2016. Addition of a
661 channel for XCO observations to a portable FTIR spectrometer for greenhouse gas measurements,
662 Atmos. Meas. Tech., 9, 2303-2313, doi:10.5194/amt-9-2303-2016

663 Hedelius, J. K., Viatte, C., Wunch, D., Roehl, C. M., Toon, G. C., Chen, J., Jones, T., Wofsy, S. C.,
664 Franklin, J. E., Parker, H., Dubey, M. K., and Wennberg, P. O., 2016. Assessment of errors and biases

665 in retrievals of X_{CO_2} , X_{CH_4} , X_{CO} , and X_{N_2O} from a 0.5 cm^{-1} resolution solar-viewing spectrometer, *Atmos.*
666 *Meas. Tech.*, 9, 3527-3546, <https://doi.org/10.5194/amt-9-3527-2016>
667 Heinle, L. and Chen, J., 2017 in review. Automated Enclosure and Protection System for Compact
668 Solar-Tracking Spectrometers, *Atmos. Meas. Tech. Discuss.*, <https://doi.org/10.5194/amt-2017-292>
669 IEA, International Energy Agency, 2008, World Energy Outlook, IEA Publications, Paris, France ISBN:
670 978926404560-6
671 IPCC-WG1, Climate Change 2013: The Physical Science Basis. Contribution of Working Group I to the
672 Fifth Assessment Report of the Intergovernmental Panel on Climate Change [Stocker, T.F., D. Qin, G.-
673 K. Plattner, M. Tignor, S.K. Allen, J. Boschung, A. Nauels, Y. Xia, V. Bex and P.M. Midgley (eds.)].
674 Cambridge University Press, Cambridge, United Kingdom and New York, NY, USA, 1535 pp
675 IPCC-WG3, Climate Change 2014: Mitigation of Climate Change. Contribution of Working Group III to
676 the Fifth Assessment Report of the Intergovernmental Panel on Climate Change [Edenhofer, O., R.
677 Pichs-Madruga, Y. Sokona, E. Farahani, S. Kadner, K. Seyboth, A. Adler, I. Baum, S. Brunner, P.
678 Eickemeier, B. Kriemann, J. Savolainen, S. Schlömer, C. von Stechow, T. Zwickel and J.C. Minx (eds.)].
679 Cambridge University Press, Cambridge, United Kingdom and New York, NY, USA
680 Janardanan, R., S. Maksyutov, T. Oda, M. Saito, J. W. Kaiser, A. Ganshin, A. Stohl, T. Matsunaga, Y.
681 Yoshida, and T. Yokota (2016), Comparing GOSAT observations of localized CO₂ enhancements by
682 large emitters with inventory-based estimates, *Geophys. Res. Lett.*, 43, 3486–3493,
683 doi:10.1002/2016GL067843.
684 Jones, N., 2013, Troubling milestone for CO₂. *Nature Geoscience* 6, no. 8, 589-589.
685 Keppel-Aleks, G., Toon, G.C., Wennberg, P.O. and Deutscher, N.M., 2007. Reducing the impact of
686 source brightness fluctuations on spectra obtained by Fourier-transform spectrometry. *Applied optics*,
687 46(21), pp.4774-4779.
688 Keppel-Aleks, G., P. O. Wennberg, and T. Schneider (2011), Sources of variations in total column
689 carbon dioxide, *Atmospheric Chemistry and Physics*, 11(8), 3581-3593, doi:10.5194/acp-11-3581-2011
690 Klappenbach, F., Bertleff, M., Kostinek, J., Hase, F., Blumenstock, T., Agusti-Panareda, A., Razinger,
691 M., and Butz, A., 2015. Accurate mobile remote sensing of XCO₂ and XCH₄ latitudinal transects from
692 aboard a research vessel, *Atmos. Meas. Tech.*, 8, 5023-5038, <https://doi.org/10.5194/amt-8-5023-2015>
693 Kort, E. A., C. Frankenberg, C. E. Miller, and T. Oda (2012), Space-based observations of megacity
694 carbon dioxide, *Geophys. Res. Lett.*, 39, L17806, doi:10.1029/2012GL052738.
695 Lauvaux, T., Miles, N.L., Deng, A., Richardson, S.J., Cambaliza, M.O., Davis, K.J., Gaudet, B.,
696 Gurney, K.R., Huang, J., O'Keefe, D. and Song, Y., 2016. High-resolution atmospheric inversion of
697 urban CO₂ emissions during the dormant season of the Indianapolis Flux Experiment (INFLUX).
698 *Journal of Geophysical Research: Atmospheres*, 121(10), pp.5213-5236.
699
700 Latoska, A., 2009. Erstellung eines räumlich hoch aufgelösten Emissionsinventar von Luftschadstoffen
701 am Beispiel von Frankreich im Jahr 2005, Master's thesis, Institut für Energiewirtschaft und Rationelle
702 Energieanwendung, Universität Stuttgart, Stuttgart, Germany
703 Levin, I., Hammer, S., Eichmann, E. and Vogel, F.R., 2011. Verification of greenhouse gas emission
704 reductions: the prospect of atmospheric monitoring in polluted areas. *Philosophical Transactions of the*
705 *Royal Society of London A: Mathematical, Physical and Engineering Sciences*, 369(1943), pp.1906-
706 1924.

Formatted: Font: (Default) Arial, 10 pt, German (Germany)

Formatted: Font: (Default) Arial, 10 pt

Formatted: Font: 10 pt

Formatted: Font: (Default) Arial, 10 pt

Formatted: Font: 10 pt

707 Messerschmidt, J., Geibel, M. C., Blumenstock, T., Chen, H., Deutscher, N. M., Engel, A., Feist, D. G.,
708 Gerbig, C., Gisi, M., Hase, F., Katrynski, K., Kolle, O., Lavrič, J. V., Notholt, J., Palm, M., Ramonet, M.,
709 Rettinger, M., Schmidt, M., Sussmann, R., Toon, G. C., Truong, F., Warneke, T., Wennberg, P. O.,
710 Wunch, D., and Xueref-Remy, I., 2011. Calibration of TCCON column-averaged CO₂: the first aircraft
711 campaign over European TCCON sites, *Atmos. Chem. Phys.*, 11, 10765-10777,
712 <https://doi.org/10.5194/acp-11-10765-2011>
713 [Mitchell, L.E., Lin, J.C., Bowling, D.R., Pataki, D.E., Strong, C., Schauer, A.J., Bares, R., Bush, S.E.,](#)
714 [Stephens, B.B., Mendoza, D. and Mallia, D., 2018. Long-term urban carbon dioxide observations reveal](#)
715 [spatial and temporal dynamics related to urban characteristics and growth. *Proceedings of the National*](#)
716 [Academy of Sciences, 115\(12\), pp.2912-2917.](#)
717 Nassar, R., Hill, T.G., McLinden, C.A., Wunch, D., Jones, D.B.A. and D. Crisp, 2017. Quantifying CO₂
718 emissions from individual power plants from space, *JGR*, 44, 19, 10045-1053.
719 Nassar, R., Napier-Linton, L., Gurney, K.R., Andres, R.J., Oda, T., Vogel, F.R. and Deng, F., 2013.
720 Improving the temporal and spatial distribution of CO₂ emissions from global fossil fuel emission data
721 sets. *Journal of Geophysical Research: Atmospheres*, 118(2), pp.917-933.
722 O'Brien, D.M., Polonsky, I.N., Utembe, S.R. and Rayner, P.J., 2016. Potential of a geostationary
723 geoCARB mission to estimate surface emissions of CO₂, CH₄ and CO in a polluted urban environment:
724 case study Shanghai. *Atmospheric Measurement Techniques*, 9(9), p.4633.
725 [Olivier, J. and G. Janssens-Maenhout, CO₂ Emissions from Fuel Combustion -- 2012 Edition, IEA CO₂](#)
726 [report 2012, Part III, Greenhouse-Gas Emissions, ISBN 978-92-64-17475-7](#)
727 Rötzer, T., and F-M. Chmielewski. 2001. Phenological maps of Europe., *Climate research* 18.3, 249-
728 257.
729 Schwandner, F.M., Gunson, M.R., Miller, C.E., Carn, S.A., Eldering, A., Krings, T., Verhulst, K.R.,
730 Schimel, D.S., Nguyen, H.M., Crisp, D. and O'dell, C.W., 2017. Spaceborne detection of localized
731 carbon dioxide sources. *Science*, 358(6360), p.eaam5782.
732 Schneider, M. and Hase, F.: Ground-based FTIR water vapour profile analyses, *Atmos. Meas. Tech.*,
733 2, 609–619, doi:10.5194/amt-2-609-2009, 2009.
734 Stauer, J., Broquet, G., Bréon, F.M., Puygrenier, V., Chevallier, F., Xueref-Rémy, I., Dieudonné, E.,
735 Lopez, M., Schmidt, M., Ramonet, M. and Perrussel, O., 2016. The first 1-year-long estimate of the
736 Paris region fossil fuel CO₂ emissions based on atmospheric inversion. *Atmospheric Chemistry and*
737 *Physics*, 16(22), pp.14703-14726.
738 [Strong, C., Stwertka, C., Bowling, D.R., Stephens, B.B. and Ehleringer, J.R., 2011. Urban carbon](#)
739 [dioxide cycles within the Salt Lake Valley: A multiple-box model validated by observations. *Journal of*](#)
740 [Geophysical Research: Atmospheres, 116\(D15\).](#)
741 Turnbull, J.C., Sweeney, C., Karion, A., Newberger, T., Lehman, S.J., Tans, P.P., Davis, K.J., Lauvaux,
742 T., Miles, N.L., Richardson, S.J. and Cambaliza, M.O., 2015. Toward quantification and source sector
743 identification of fossil fuel CO₂ emissions from an urban area: Results from the INFLUX experiment.
744 *Journal of Geophysical Research: Atmospheres*, 120(1), pp.292-312.

Formatted: Font: 10 pt

Formatted: Font: 10 pt

Formatted: Font: 10 pt

745 [Vogel, F.R., Ishizawa, M., Chan, E., Chan, D., Hammer, S., Levin, I. and Worthy, D.E.J., 2012. Regional](#)
746 [non-CO2 greenhouse gas fluxes inferred from atmospheric measurements in Ontario, Canada. *Journal*](#)
747 [of Integrative Environmental Sciences, 9\(sup1\), pp.41-55.](#)
748 Vogel, F.R., Thiruchittampalam, B., Theloke, J., Kretschmer, R., Gerbig, C., Hammer, S. and Levin, I.,
749 2013. Can we evaluate a fine-grained emission model using high-resolution atmospheric transport
750 modelling and regional fossil fuel CO2 observations?. *Tellus B: Chemical and Physical Meteorology*,
751 65(1), p.18681.
752 Wunch, D., Toon, G.C., Blavier, J.F.L., Washenfelder, R.A., Notholt, J., Connor, B.J., Griffith, D.W.T.,
753 Sherlock, V. and Wennberg, P.O., 2011. The total carbon column observing network, *Philos. T. Roy.*
754 *Soc. A*, 369, 2087–2112.
755 Wunch, D., Toon, C., Wennberg, O., Wofsy, C., Stephens, B., Fischer, L., Uchino, O., Abshire, B.,
756 Bernath, P., Biraud, C. and Blavier, F., 2010. Calibration of the total carbon column observing network
757 using aircraft profile data. *Atmospheric Measurement Techniques*, 3(5), pp.1351-1362.
758 Xueref-Remy, I., Dieudonné, E., Vuillemin, C., Lopez, M., Lac, C., Schmidt, M., Delmotte, M., Chevallier,
759 F., Ravetta, F., Perrussel, O., Ciais, P., Bréon, F.-M., Broquet, G., Ramonet, M., Spain, T. G., and
760 Ampe, C.: Diurnal, synoptic and seasonal variability of atmospheric CO2 in the Paris megacity area,
761 [Atmospheric Chemistry and Physics, 18\(5\), pp.3335-3362. *Atmos. Chem. Phys. Discuss.*,](#)
762 <https://doi.org/10.5194/acp-2016-218>, accepted in ACP.

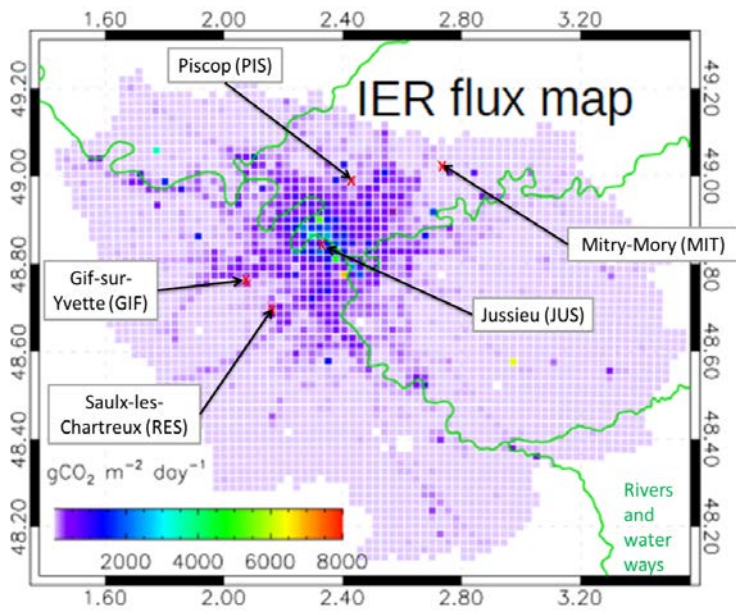
Formatted: Font: 10 pt

Formatted: pb_toc_link, Font: 10 pt, Not Italic

Formatted: pb_toc_link, Font: 10 pt

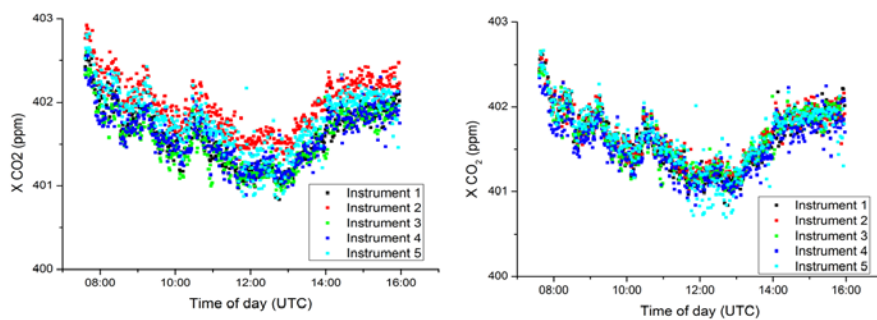
Formatted: pb_toc_link, Font: 10 pt, Not Italic

Formatted: pb_toc_link, Font: 10 pt

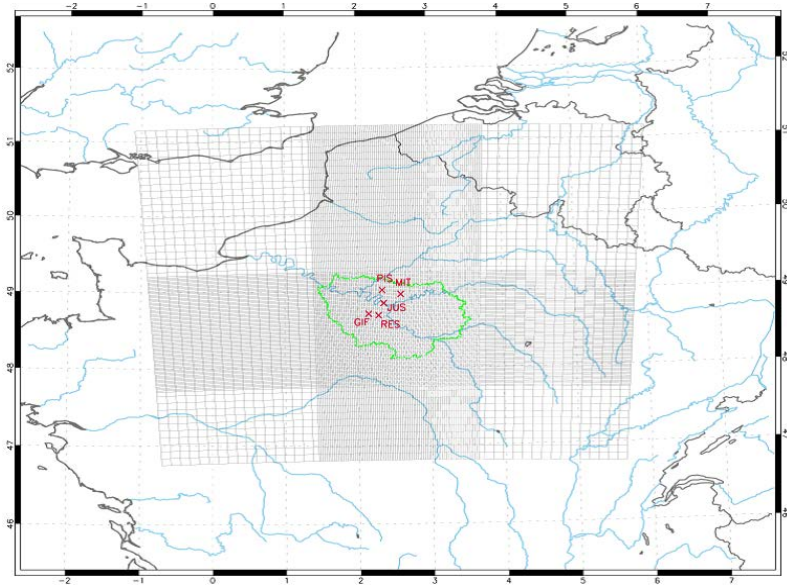


763
764
765

Figure 1. CO₂ emissions in the Île-de-France region according to the IER emission inventory. Measurement sites are indicated by red crosses.

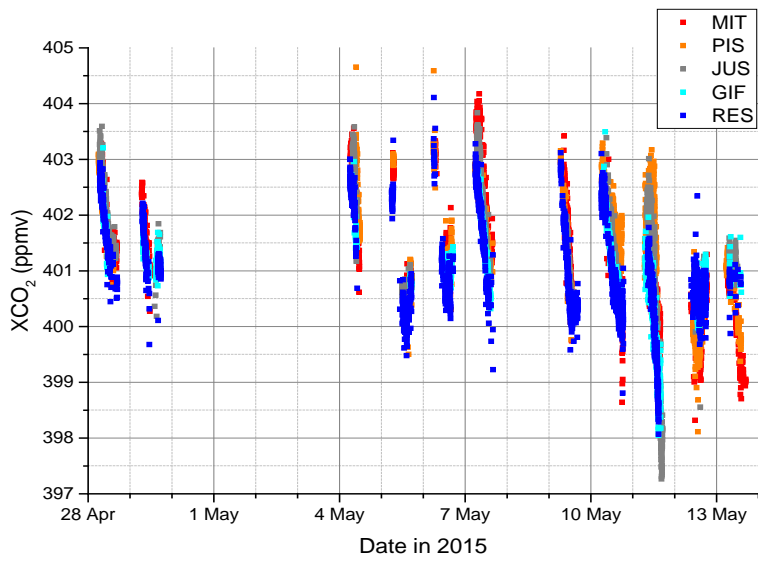


766
767 **Figure 2. Sample parallel measurements of the five EM27/SUN instruments in Karlsruhe**
768 **for raw data (left panel) and the data with the applied correction (right panel) taken on**
769 **April 15th, 2015.**



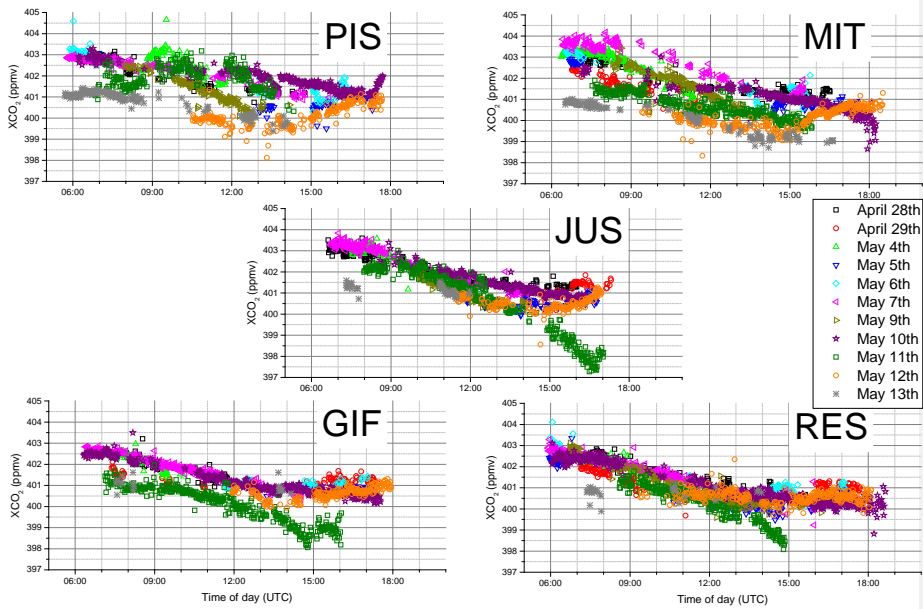
770
771
772

Figure 3. Modelling domain and numerical grid configuration of CHIMERE with a zoom on the Ile-de-France region at 2 x 2 km².



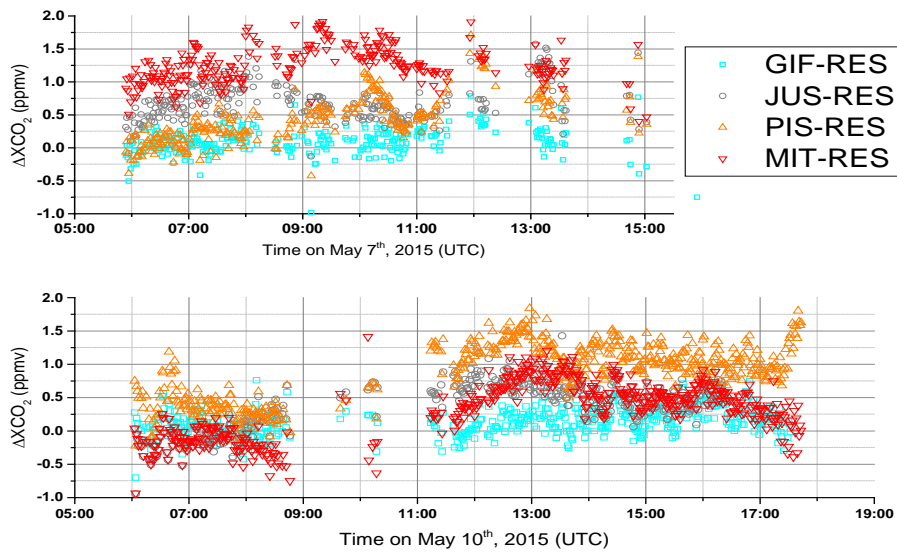
773
774
775

Figure 42. Time series of observed XCO₂ in the Parisian region for all five sites (all valid data of ~ 1 minute averages).



776
777

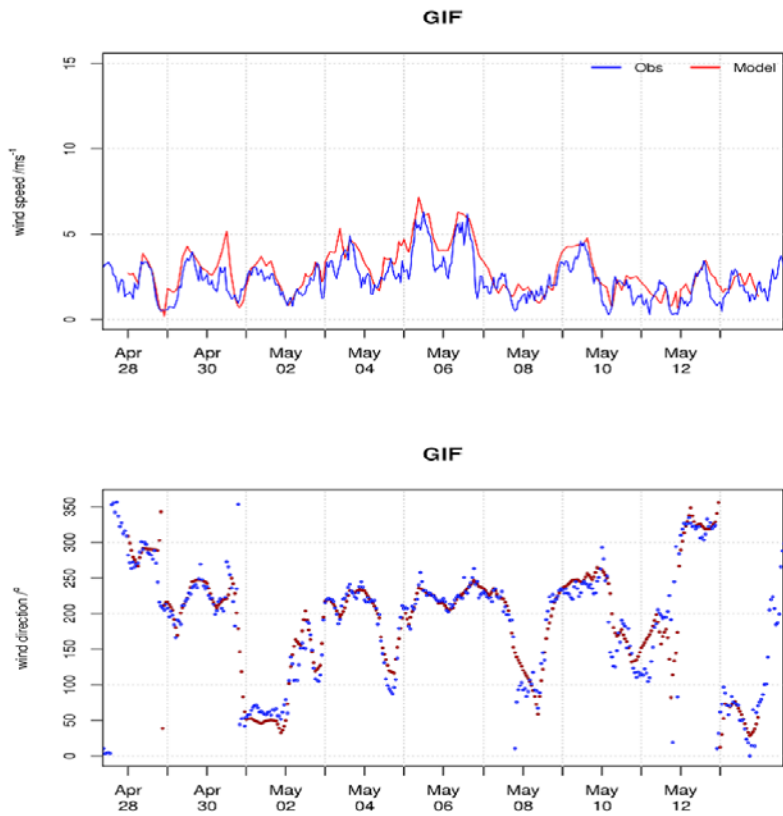
Figure 35. Time series of observed XCO₂ in the Parisian region sorted by station.



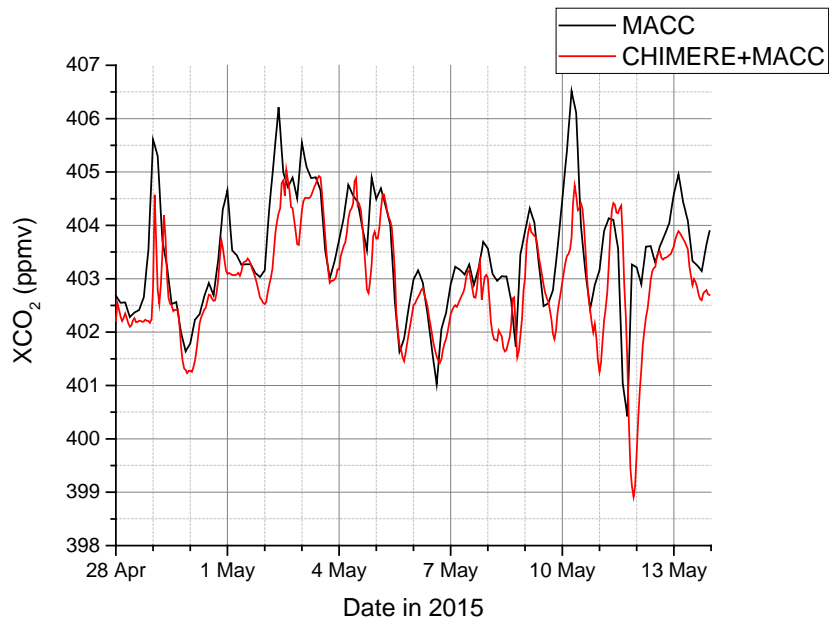
778
779
780

Figure 46. Observed spatial gradients of XCO₂ for May 7th (southwesterly winds) and May 10th (southerly winds).

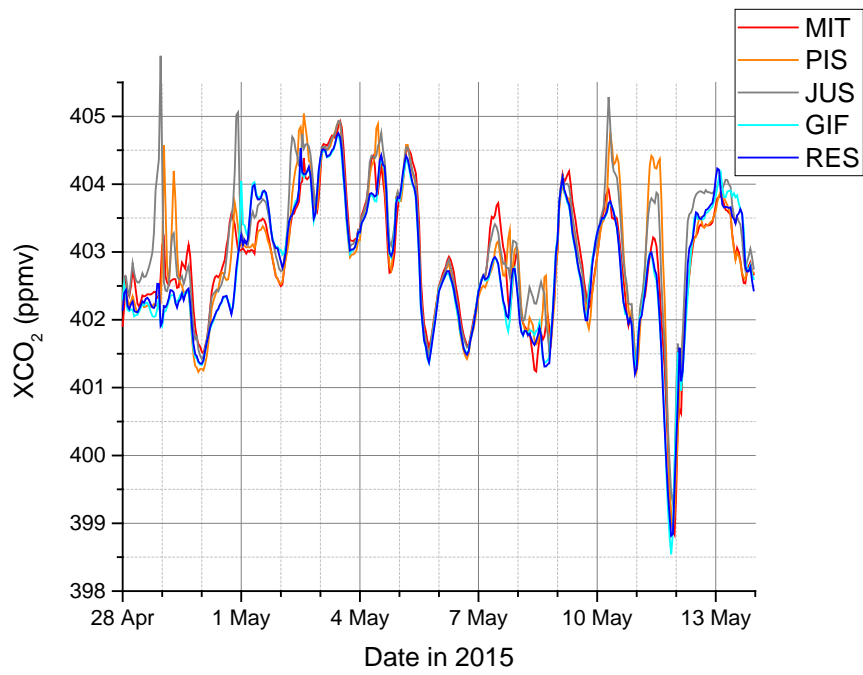
Formatted: Superscript
Formatted: Superscript



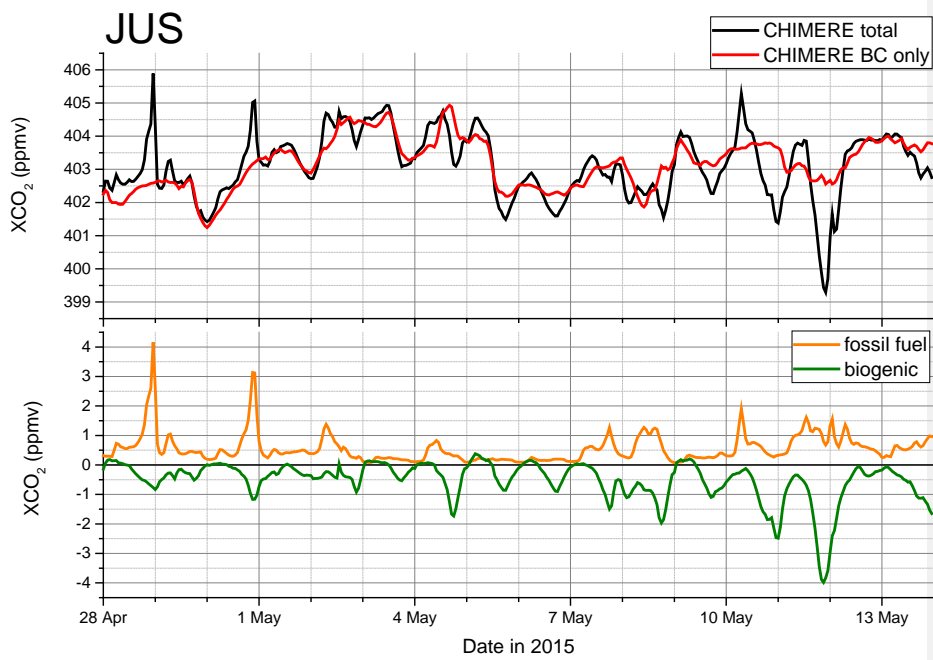
781
 782 **Figure 7. Comparison of modelled and observed wind speeds and directions at the Gif-**
 783 **Sur-Yvette measurement site**



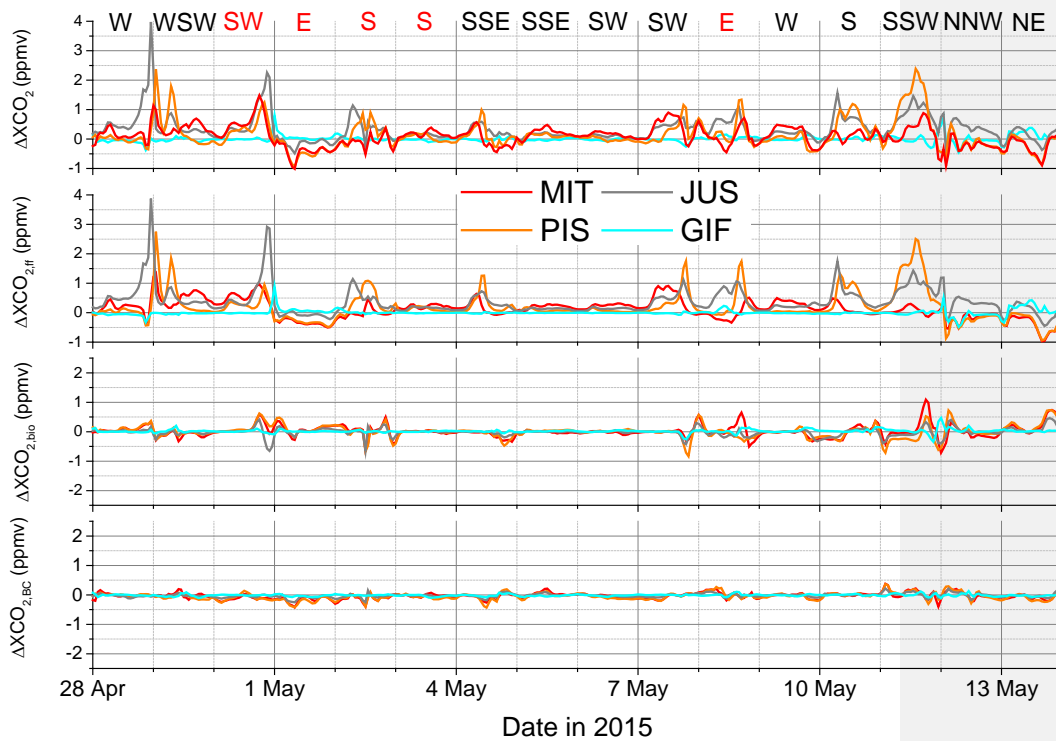
784
 785 **Figure 8. Comparison of modelled XCO₂ from ECWMF-CAMS (15 x 15 km²) with**
 786 **CHIMERE simulation (inner domain, 2 x 2 km²) for JUS.**



787
788 **Figure 59. Modelled XCO₂ for all stations.**

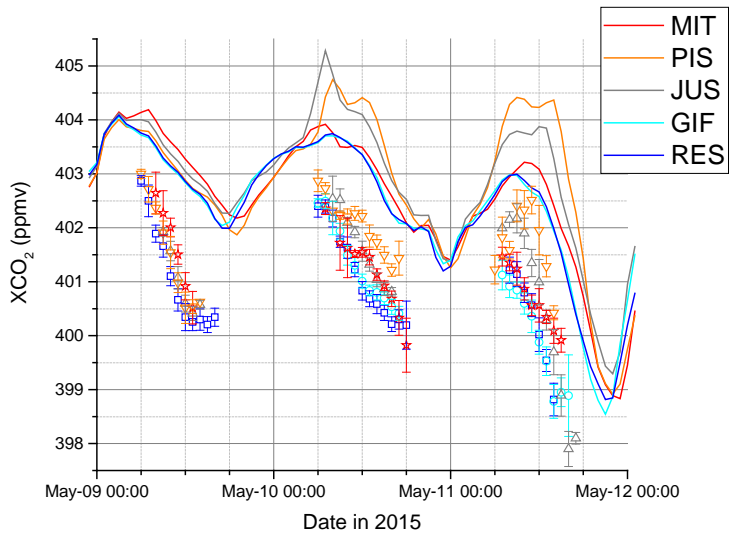


789
 790 **Figure 406:** Time series of XCO₂ and related fluxes for JUS. The top panel provides a comparison of modelled total XCO₂ and XCO₂ variations due to changes in boundary conditions **(BC only)**. The lower panel shows the contribution of the different flux components, namely fossil fuel CO₂ emissions and biogenic fluxes.
 792
 793

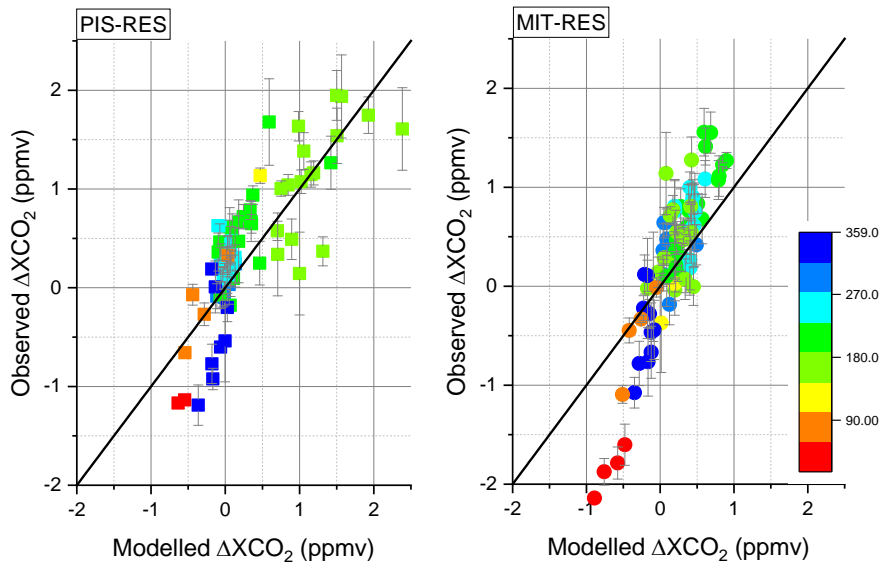


794
 795 **Figure 447. Modelled XCO₂ gradients for each station relative to RES are given in the**
 796 **top panel with its contributing components in the panels below. -Total ΔXCO_2 (top), the**
 797 **fossil fuel contribution $\Delta XCO_{2,ff}$ (second from top), the biogenic contribution $\Delta XCO_{2,bio}$**
 798 **(third from top) and the influence of the boundary conditions, $\Delta XCO_{2,BC}$ (bottom). The**
 799 **dominant wind conditions for each day given at the top of the figure and days without**
 800 **observations due to precipitation are in red.**

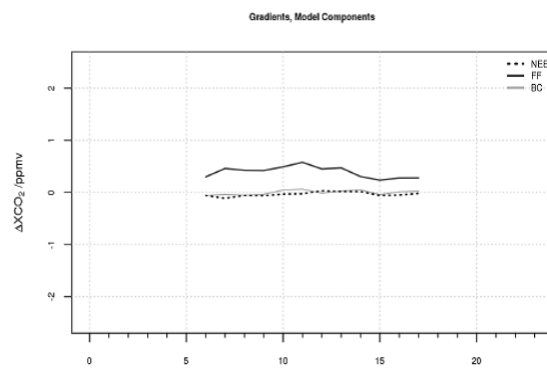
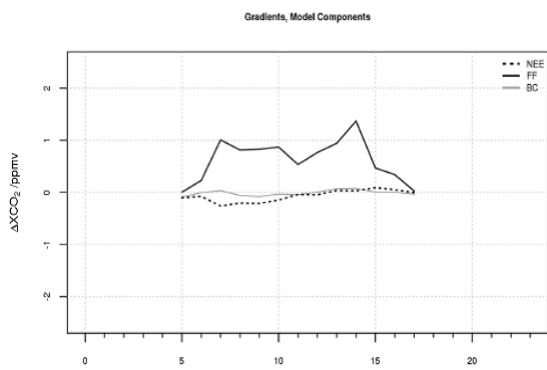
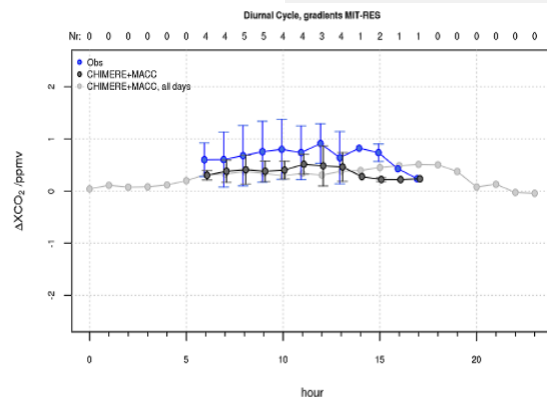
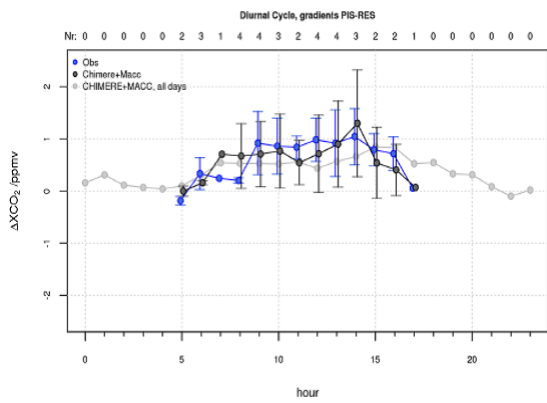
- Formatted: Font: Symbol
- Formatted: Subscript
- Formatted: Font: Symbol
- Formatted: Font: Symbol
- Formatted: Subscript
- Formatted: Font: Symbol
- Formatted: Subscript



801
 802 **Figure 428.** Comparison of modelled (solid lines) and observed hourly averaged XCO₂
 803 (symbols) with standard deviations as error bars.



804
 805 **Figure 439.** Comparison of modelled and observed hourly averaged ΔXCO_2 for
 806 gradients between PIS and RES (left) and MIT and RES (right), with standard deviations
 807 of the minute values of the hourly mean as vertical bars and the points color coded by
 808 wind direction from 0 to 359 degrees.



809
 810 **Figure 4410.** Comparison of modelled (black) and observed mean daily cycle (blue) of
 811 hourly averaged ΔXCO_2 of PIS with RES (top left) and of MIT with RES (top right) during
 812 the campaign when RES can be considered as upwind site. Labels on top of the upper
 813 figures denote the number of days contributing to the mean. The mean daily cycle for
 814 all days within the campaign period when PIS and MIT are downwind of RES is given in
 815 light grey and the modelled contribution of different CO₂ sources/sinks to the mean
 816 daily cycle for days with observations for the two sites is given in the (bottom panels).

Location	ID	Lat (deg)	Lon (deg)	Position
Piscep	PIS	49.019	2.347	20 km NNW of JUS
Mitry-Mory	MIT	48.984	2.626	25 km NW of JUS
Jussieu	JUS	48.846	2.356	Paris city centre
Saulx-les-Chartreux	RES	48.688	2.284	20 km SSW of JUS
Gif-Sur-Yvette	GIF	48.708	2.148	20 km SW of JUS

Table 1. Location of FTIR measurement instruments during the field campaign

Instrument	XCO ₂ factor Berlin	XCO ₂ factor before Paris	XCO ₂ factor after Paris
1	1.0000 (0.0003)	1.0000 (0.0003)	1.0000 (0.0003)
2	0.9992 (0.0003)	0.9991 (0.0003)	0.9992 (0.0003)
3	1.0002 (0.0003)	1.0001 (0.0004)	1.0000 (0.0005)
4	0.9999 (0.0003)	1.0000 (0.0004)	1.0000 (0.0004)
5	0.9996 (0.0003)	0.9995 (0.0003)	0.9995 (0.0003)

818 Table 21. Normalisation factors for the five EM27/SUN instruments derived during
 819 measurements before and after the Paris field campaign. Values in parentheses are
 820 standard deviations. Measurements of instrument 1 were arbitrarily chosen as
 821 reference from which the others were scaled. The calibration factors from a previous
 822 field campaign in Berlin [Hase et al. 2015] are also shown. Calibration factors between
 823 the two field campaigns agree well within 0.02 % (~0.08 ppm) for all instruments.

Date	No. of observations					Quality	Wind speed (m s ⁻¹)	Wind direction
	MIT	GIF	PIS	RES	JUS			
28 Apr 2015 (Tu)	179	102	178	199	234	++	4	W
29 Apr 2015 (We)	110	124	0	161	53	+	5	SW-W
04 Mai 2015 (Mo)	194	85	96	163	83	+	6	S-SE
05 Mai 2015 (Tu)	77	27	85	185	92	+	8	S-SW
06 Mai 2015 (We)	81	88	87	139	0	+	8	SW
07 Mai 2015 (Th)	169	313	252	286	238	+++	3	SW
09 Mai 2015 (Sa)	179	0	181	289	149	++	6	W
10 Mai 2015 (Su)	325	478	362	542	282	++++	3	S
11 Mai 2015 (Mo)	410	431	251	298	413	++++	3	SSW
12 Mai 2015 (Tu)	324	222	230	326	203	+++	4	NNW
13 Mai 2015 (We)	159	18	182	28	56	+	4	NE

824 Table 32. Summary of all measurement days with the number of observations at each
825 of the sites, Mitry Mory (MIT) , Gif Sur Yvette (GIF), Piscop (PIS), Saulx-les-Chartreux
826 (RES), Jussieu (JUS), the overall quality ranking of each day according to the number
827 of available observations –and temporal coverage (with classification from poor to
828 great: +, ++, +++, +++++), and the ground-level wind speed and direction.

	Total-obs	Mean (ppm)	STD (ppm)	Quartile1 (ppm)	Median (ppm)	Quartile3 (ppm)
RES	2616	401.11	0.93	400.44	400.88	401.96
GIF	1888	401.05	0.92	400.94	400.94	401.58
JUS	1803	401.33	1.17	401.31	401.31	402.04
PIS	1904	401.62	0.95	401.03	401.59	402.44
MIT	2207	401.26	1.15	401.11	401.11	401.95

Table 4. Statistics of observed XCO₂ 1-minute averages for all sites

829